Smart Agricultural Technology 14 (2026) 102271

Contents lists available at ScienceDirect

Smart Agricultural Technology

journal homepage: www.journals.elsevier.com/smart-agricultural-technology

Modeling the potential distribution of *Musa* (AAB), cv. 'Bellaco' and *Carica papaya* under climate change scenarios in the provinces of Jaén and San Ignacio

Jefferson A. Cubas Sanchez [a,*], Beimer Chuquibala-Checan [a], Nilton Atalaya-Marin [a], Daniel Tineo [a], Victor H. Taboada-Mitma [a], Héctor Cabrera-Hoyos [b], Juancarlos Cruz-Luis [c], Malluri Goñas [a], Darwin Gómez-Fernández [a]

[a] Centro Experimental Yanayacu, Dirección de Servicios Estratégicos Agrarios (DSEA), Instituto Nacional de Innovación Agraria (INIA), Carretera Jaén San Ignacio km 23.7, Jaén 06801, Perú
[b] Estación Experimental Agraria Baños del Inca, Dirección de Servicios Estratégicos Agrarios (DSEA), Instituto Nacional de Innovación Agraria (INIA), Jirón Wiracocha S/N, Cajamarca 06001, Perú
[c] Dirección de Servicios Estratégicos Agrarios (DSEA), Instituto Nacional de Innovación Agraria (INIA), Av. La Molina 1981, Lima 15024, Perú

ARTICLE INFO

Keywords:
Suitability
MaxEnt
Shared socioeconomic pathways (SSP)
Crops

ABSTRACT

Plantain (*Musa* (AAB), cv. 'Bellaco') and papaya (*Carica papaya*) are key crops for the economy and food security in northwestern Peru; however, the lack of spatially explicit information on their current and future suitability limits agricultural planning and climate change adaptation. This study modeled the current and future potential distribution (2050 and 2070) of both crops in the provinces of Jaén and San Ignacio under the SSP1– 2.6, SSP2– 4.5, and SSP5– 8.5 scenarios, using 262 occurrence records for plantain and 125 for papaya, together with bioclimatic, edaphic, and topographic predictors standardized to a spatial resolution of 1 km. MaxEnt models calibrated with 25-fold cross-validation showed excellent performance (current AUC = 0.922–0.928; projected AUC = 0.957–0.965). The main predictors were elevation (58.97%), precipitation of the coldest quarter (Bio19, 13.39%), and silt content (7.55%) for plantain, and temperature seasonality (Bio4, 82.06%) for papaya. Projections indicate a marked spatial redistribution for both crops. Although between 78.93% and 85.92% of the territory remained in the same suitability class, plantain showed consistently negative net balances across all scenarios, with losses of up to −1690.87 km^2 under SSP5– 8.5 in 2070. For papaya, some scenarios showed short-term gains in high-suitability areas (up to 26.50% in 2050), but by 2070 net losses predominated, reaching −34.59% under SSP5– 8.5. These findings reveal crop-specific patterns that are overall unfavorable under climate change and provide a spatial basis for crop zoning, territorial prioritization, and the planning of adaptation measures aimed at site selection, crop diversification, and water management.

1. Introduction

Fruticulture constitutes an important economic activity for the development of tropical and subtropical regions. Crops such as plantain (*Musa* (AAB), cv. 'Bellaco') and papaya (*Carica papaya*) represent important sources of income and food security worldwide [1–4]. In northwestern Peru, specifically in the provinces of Jaén and San Ignacio in the department of Cajamarca, after coffee, cacao and rice as flagship products, these crops are established as growing sources of income for small farmers [5]. At the regional scale, plantain production is concentrated mainly in Jaén and San Ignacio, with reported annual production in 2025 of 17,737.63 t and 15,863.00 t, respectively, and farm-gate prices of S/ 0.94 kg^{-1} and S/ 0.71 kg^{-1} [5]. Likewise, papaya is increasingly integrated into local fruit production systems as a complementary cash crop, with reported production of 674.11 t in Jaén and 889.93 t in San Ignacio, and farm-gate prices of S/ 1.60 kg^{-1} and S/ 1.32 kg^{-1}, respectively, thereby strengthening household profitability through diversification and market supply [5].

Climate change is increasingly compromising the sustainability of agricultural systems by altering key variables such as temperature and

* Corresponding author at: Jaén 06801, Cajamarca, Perú.
E-mail address: jeffersoncubas3012@gmail.com (J.A. Cubas Sanchez).

https://doi.org/10.1016/j.atech.2026.102271
Received 29 December 2025; Received in revised form 17 March 2026; Accepted 1 June 2026
Available online 6 June 2026

precipitation, thereby affecting crop productivity, production stability, and food security [6–9]. In particular, the increasing frequency and intensity of extreme events, including droughts, heat waves, and intense rainfall, can reduce yields, accelerate soil degradation, and disrupt food supply and price stability, with particularly severe consequences for vulnerable agricultural systems and food-import-dependent regions [10–12]. Although adaptation measures such as irrigation or management adjustments may partially buffer these impacts, their effectiveness remains variable across crops, production systems, and regions, and the extent to which adaptation can offset future losses remains uncertain [13–15]. In this context, generating evidence on how climate change may alter the suitability of strategic crops is essential to support agricultural planning, adaptation, and long-term resilience.

Northwestern Peru exhibits high climate vulnerability because exposure to droughts, intense rainfall, and thermal variability occurs across a landscape characterized by steep altitudinal and hydroclimatic gradients [16–18]. In Jaén and San Ignacio, precipitation generally increases with elevation and shows pronounced spatial contrasts, whereas mean annual temperature decreases with altitude, creating distinct agroclimatic zones with differentiated production responses [19]. This heterogeneity constrains water availability, modulates the length of the growing period, and increases crop susceptibility to water stress, soil erosion, and flooding [19]. Moreover, in smallholder agricultural systems, land fragmentation, limited irrigation infrastructure, and reliance on rainfall heighten production sensitivity and amplify the volatility of rural incomes [20].

Each fruit crop possesses specific requirements regarding climatic conditions that influence its growth, development, and production. Plantain, for example, requires constant high temperatures that range between 26 and 30 °C, annual precipitation between 1500 and 2500 mm, and relative humidity levels above 60% [21,22]. Papaya requires conditions similar to those of plantain; however, it is sensitive to prolonged periods of drought or excess water [23,24]. This diversity of requirements, combined with the region's altitude heterogeneity, highlights the importance of identifying areas with optimal conditions for each crop.

Against this backdrop, the assessment of climatic suitability using Species Distribution Models (SDMs) constitutes a strategic tool for identifying suitable areas, anticipating geographic shifts in crop distribution, and supporting agricultural planning under climate change [25,26]. In particular, Maximum Entropy (MaxEnt) has been widely applied to model the potential distribution of crops and other agriculturally important species under current conditions and climate change scenarios [27]. Studies on coffee and mango have used this approach to project changes in suitability, identify key climatic drivers, and inform adaptation and land-use planning decisions [28,29]. Similarly, applications in cacao have demonstrated the value of these approaches for anticipating shifts in climatic suitability and supporting adaptation strategies in producing regions [30]. In Peru, studies integrating MaxEnt, AHP, and GIS have further confirmed its usefulness for delineating favorable areas and informing agricultural zoning strategies [31]. In addition, these approaches make it possible to assess how changes in temperature and precipitation may shift suitable areas, for example, toward higher elevations [32–34].

The integration of MaxEnt in R through specialized packages allows automating tasks [35], facilitating calibration and its application in studies directed at evaluating and projecting the impact of climate change on the current and future distribution of crops [36]. Nevertheless, a recurrent limitation is the excessive dependence on bioclimatic variables, since it generates biases in territories with high environmental variability [37–39]. In these contexts, the delimitation of suitable areas is usually based on environmental zonations constructed from exploratory analyses of topographic, bioclimatic, and edaphic variables [40].

Despite these advances, limited information is available on the current and future climatic suitability of plantain and papaya in northwestern Peru under contrasting SSP scenarios. Therefore, this study employs the MaxEnt model to evaluate the current and future climatic suitability of two priority fruit crops (plantain and papaya) in northwestern Peru, a region with high agricultural productivity and elevated vulnerability to climate change. For this purpose, historical climatic data and projections under the SSP1– 2.6, SSP2– 4.5, and SSP5– 8.5 scenarios were used for the periods 2041–2060 (2050) and 2061–2080 (2070), with which the geographical distribution of suitable areas for these crops was modeled. This study identifies the climatic suitability of each crop and provides comparative maps between current and future conditions. Consequently, it offers a replicable tool that supports agricultural planning and the adaptation of crops to climate change, and contributes to more resilient agriculture in the face of climate change scenarios.

2. Materials and methods

The methodological workflow of this study is shown in Fig. 1, which integrates data collection, analysis, and evaluation for modeling the potential distribution of plantain and papaya under current and future climate scenarios in the provinces of Jaén and San Ignacio.

2.1. Study area

The study area comprises the provinces of Jaén and San Ignacio, in the department of Cajamarca, northwestern Peru (Fig. 2). This territory is characterized by marked environmental heterogeneity, forming a mosaic of ecological conditions associated with wide altitudinal gradients, complex topography, the presence of inter-Andean valleys, and contrasting hydroclimatic conditions, which generate considerable spatial variation in temperature and precipitation [41]. This environmental diversity directly conditions the distribution of crops and is fundamental for assessing their suitability in the face of climate change.

The province of Jaén presents altitudes from 333 to 3963 m a.s.l [42]; with mean annual temperatures between 11 and 33 °C, precipitation between 350 and 1000 mm, and relative humidity between 65% and 84% [43]. It has an area of 5232.57 km^2 [44], of which 31% is dedicated to agricultural activity [45], and is home to a population of 185,432 inhabitants [46], of whom 1079 are plantain growers and 164 are papaya growers [5].

For its part, the province of San Ignacio has altitudes between 352 and 3799 m a.s.l [42], with mean annual temperatures between 11 and 29 °C and annual precipitation varying between 700 and 3500 mm [43]. Its territorial extension reaches 4990.30 km^2 [47], with 32% of its surface area oriented towards agriculture [45]. Its population is 130,620 inhabitants [46], with 1411 dedicated to plantain cultivation and 61 to papaya cultivation [5].

2.2. Occurrence records

Following the methodological framework outlined in Fig. 1, occurrence records for both crops were compiled and processed. Occurrence records for plantain and papaya were compiled from three complementary sources: bibliographic reports, the Global Biodiversity Information Facility database (GBIF, http://www.gbif.org), and georeferenced field records collected in cultivated areas. This combination was adopted to maximize spatial coverage across the study area through the integration of complementary occurrence sources, as well as to contrast secondary records with direct observations and improve the consistency of the dataset used for modeling [48,49]. Because online repositories may include duplicated records and georeferencing inaccuracies, all records were subjected to a cleaning and filtering process prior to model calibration [50,51].

The records were filtered to the study area and duplicate coordinates were removed, resulting in 571 and 207 unique records for plantain and papaya, respectively (Tables S1 and S2). Subsequently, spatial filtering was performed using a 1 km × 1 km raster mask, matching the spatial

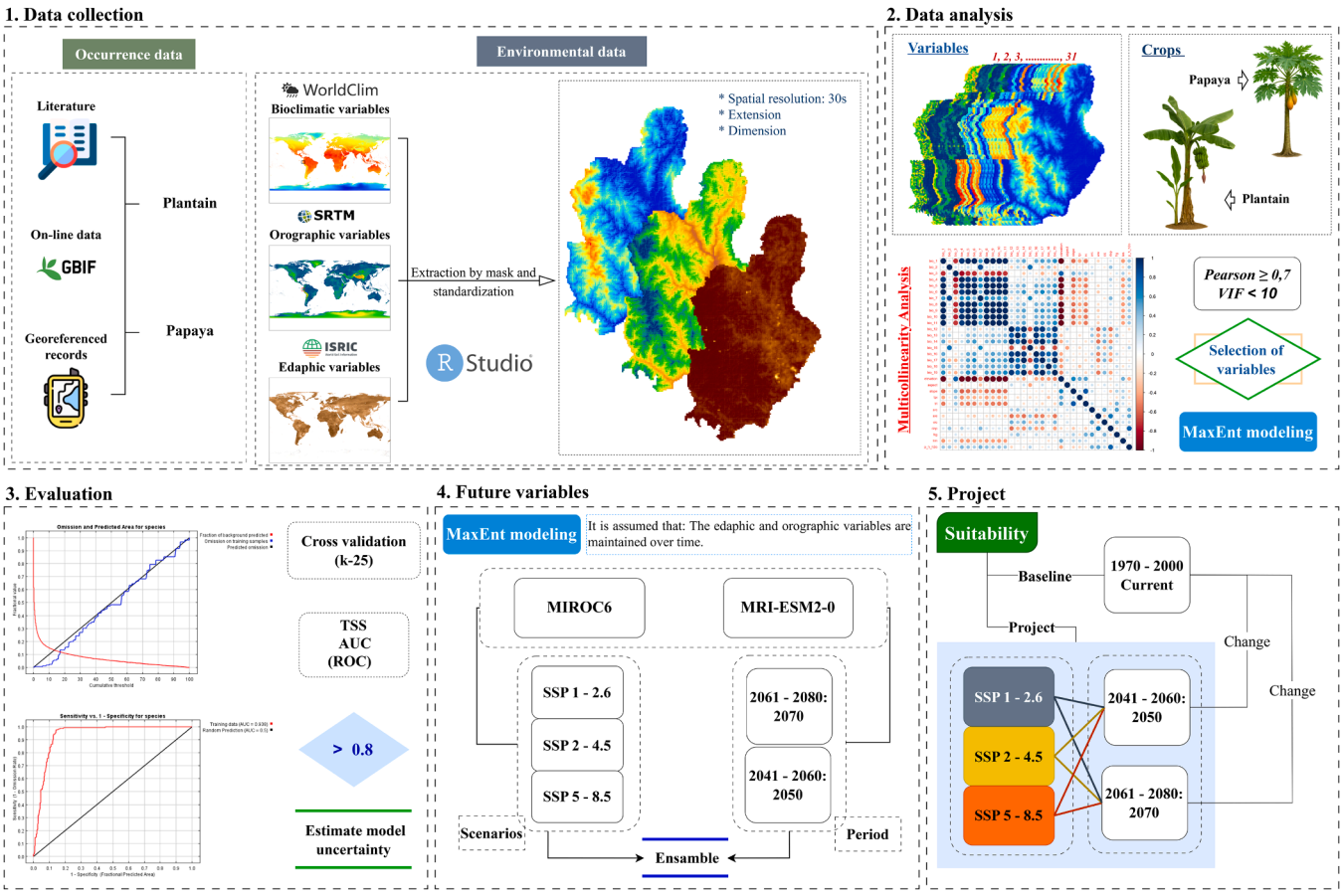

Fig. 1. Flowchart of the species distribution modeling and spatial analysis approach.

resolution of the environmental variables (~30 arc-seconds), in order to reduce spatial redundancy, minimize oversampling bias in densely sampled areas, and limit the effects of spatial autocorrelation on model performance [52–54]. The raster cell corresponding to each presence point was identified, and duplicate occurrences within the same cell were removed in R using dplyr (tidyverse package), retaining a single point per cell. This procedure is consistent with spatial filtering approaches applied to occurrence records in species distribution modeling to reduce spatial sampling bias and improve the suitability of records for model calibration and evaluation [55]. After spatial filtering, the final dataset comprised 262 records for plantain and 125 for papaya (Fig. 2).

To characterize the environmental contrast, a set of pseudo-absence points was randomly generated, excluding cells with confirmed presences. For each species, a 10:1 ratio of pseudo-absences to presences was adopted in order to reduce overfitting and maintain the model's discriminative capacity between presence and absence areas [37,50]. Although these pseudo-absences do not represent verified crop absence, they provide an operational environmental contrast for regional suitability modeling.

2.3. Environmental data

The spatial distribution of crops is shaped by the interaction of environmental variables that influence their establishment, development, and productive performance [56,57]. Among these, the bioclimatic variables temperature and precipitation are key determinants of crop growth and agricultural production [58]. However, in heterogeneous tropical landscapes such as the provinces of Jaén and San Ignacio, which are characterized by strong altitudinal gradients and complex terrain, suitability does not depend on climate alone. Edaphic properties modulate water availability, soil aeration, and other soil conditions relevant to plant growth [59,60], whereas topographic characteristics influence drainage, exposure, and local microclimatic heterogeneity [61,62]. Therefore, including edaphic and topographic variables helps overcome the limitations of purely climatic models and improves the ecological realism of projections in environmentally complex territories [27,63].

To model crop suitability, 19 bioclimatic variables from WorldClim v2.1 (http://worldclim.org; accessed March 31, 2025) [64] were integrated and automatically downloaded for Peru using the worldclim_country() function from the geodata package in R v4.4.3 [65]. In addition, seven edaphic variables were obtained from SoilGrids v2.0 (https://soilgrids.org/; accessed April 10, 2025) [66,67], and five topographic variables aspect, slope, topographic position index (TPI), and terrain ruggedness index (TRI) [33] were derived from the SRTM Digital Elevation Model (https://srtm.csi.cgiar.org; accessed May 29, 2025) [68], which was automatically downloaded using the elevation_30s() function from the geodata package. All environmental variables (Table 1) were clipped to the study area boundary and standardized to a spatial resolution of 30 arc-seconds (~1 km^2).

2.4. Multicollinearity analysis

To minimize the adverse effects of collinearity among environmental variables on the model's predictive accuracy, a statistical analysis was conducted in R v4.4.3 [65]. Pearson correlation coefficients (r) were calculated among the 31 environmental variables [35,37,56]. For pairs of variables with $|r| > 0.70$, the variable with the greater contribution was retained [58,69], and a correlation matrix was generated (Fig. 3a and b). This threshold was selected following standard practices in niche modeling to balance redundancy reduction with the retention of ecologically meaningful information [70,71].

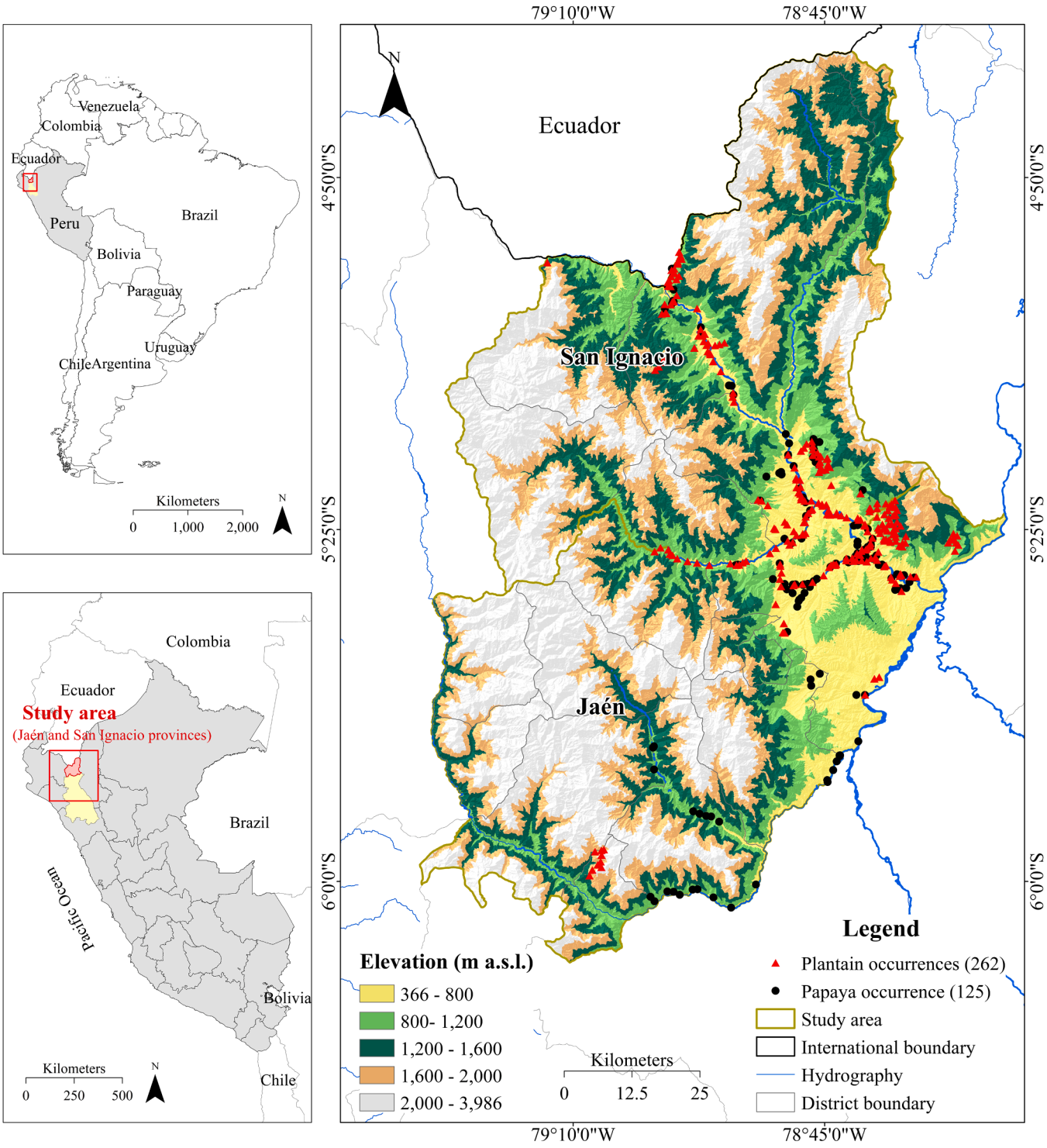

Fig. 2. Study area and occurrence points of plantain and papaya.

Subsequently, the Variance Inflation Factor (VIF) method was applied [6] using the vifstep function from the usdm package in R [72], with a variable removal threshold set at VIF $>$ 10 [35,37], a value indicative of problematic collinearity [6,70]. This procedure allowed the retention of a predictor set with low statistical redundancy but high ecological relevance for modeling plantain and papaya suitability.

2.5. Model validation

The predictive capacity of the models was evaluated by means of k-fold cross-validation in 25 folds (k = 25) on presences and pseudo-absences [73]. This strategy allowed the model to be trained with approximately 96% of the available data in each iteration, reserving the remaining 4% for independent evaluation. This methodology was chosen to maximize the use of the available data and to reduce both bias and variance in the evaluation [74]. To evaluate model performance, the Area Under the Curve (AUC) derived from the ROC curve was used [75], and the optimal threshold was determined using the TSS metric, which maximizes the sum of sensitivity and specificity [76].

The performance of the models was classified as invalid prediction

Table 1
Variables used in the prediction of the models.

Category	Code	Environmental variables	Units
Bioclimatic	Bio1	Average annual temperature	°C
	Bio2	Mean diurnal range (monthly mean of maximum temperature − minimum temperature)	°C
	Bio3	Isothermality (BIO2/BIO7) (×100)	%
	Bio4	Temperature seasonality (standard deviation ×100)	%
	Bio5	Maximum temperature of the warmest month	°C
	Bio6	Minimum temperature of the coldest month	°C
	Bio7	Annual temperature range (BIO5–BIO6)	°C
	Bio8	Mean temperature of the wettest quarter	°C
	Bio9	Mean temperature of the driest quarter	°C
	Bio10	Mean temperature of the warmest quarter	°C
	Bio11	Mean temperature of the coldest quarter	°C
	Bio12	Annual precipitation	mm
	Bio13	Precipitation of the wettest month	mm
	Bio14	Precipitation of the driest month	mm
	Bio15	Precipitation seasonality (coefficient of variation)	%
	Bio16	Precipitation of the wettest quarter	mm
	Bio17	Precipitation of the driest quarter	mm
	Bio18	Precipitation of the warmest quarter	mm
	Bio19	Precipitation of the coldest quarter	mm
Topographic	Elev	Elevation	m
	Asp	Aspect	°
	Pen	Slope	°
	TPI	Topographic position index	-
	TRI	Terrain ruggedness index	-
Edaphic	CIC	Cation exchange capacity of the topsoil layer	cmol (+)/kg
	Arc	Clay content in the topsoil layer	%
	Are	Sand content in the topsoil layer	%
	Lim	Silt content in the topsoil layer	%
	Dap	Reference bulk density of the topsoil layer	g/cm³
	Frg	Coarse fragment content in the topsoil layer	%
	pH_H2O	Measure of soil acidity or alkalinity, based on the concentration of H^+ ions	pH

(0.50 ≤ AUC < 0.60), poor prediction (0.60 ≤ AUC < 0.70), fair prediction (0.70 ≤ AUC < 0.80), good prediction (0.80 ≤ AUC < 0.90), and excellent prediction (0.90 ≤ AUC ≤ 1) [77,78]. Additionally, the relative importance of each environmental variable was quantified by means of extracting the percentage contribution from the results generated by MaxEnt. The values obtained for AUC, TSS thresholds, and the contribution of the variables were organized into tables exported in CSV format to facilitate further analyses.

2.6. Uncertainty in model results

The uncertainty of the model for current conditions was quantified using the standard deviation of an ensemble of 25 suitability models generated by means of k-fold cross-validation (k = 25) [6]. Each model was calibrated and projected independently using distinct data subsets for training and validation. The standard deviation was calculated from the stacked raster of the 25 individual projections to represent the variability among the replicates [37], where higher values indicate greater model uncertainty. Previously, all replicates were aligned to the same cell grid and masked consistently with the study area to ensure spatial comparability [79]. Finally, the standard deviation values were rescaled to a range from 0 to 100 to facilitate the interpretation and comparison of relative uncertainty across the study area [37].

2.7. Future environmental variables

To assess future climate projections, two General Circulation Models (GCMs) from the Coupled Model Intercomparison Project Phase 6 (CMIP6) were used: MIROC6 [80] and MRI-ESM2– 0 [81]. Model selection was based on four criteria: (i) their equilibrium climate sensitivity (ECS) falls within the likely range assessed in the IPCC AR6 (2.5–4.0 °C; MIROC6: 2.61 °C; MRI-ESM2– 0: 3.15 °C), thereby reducing the risk of biases associated with models exhibiting extreme sensitivities [82]; (ii) they have shown reasonable performance in simulating temperature and precipitation patterns, including evaluations in tropical and humid environments within the CMIP6 ensemble [83,84]; (iii) they belong to different model families, which helps capture part of the structural uncertainty inherent to climate simulations [85]; and (iv) due to computational limitations associated with processing multiple scenarios at 1 km resolution, a reduced number of models was prioritized.

Three Shared Socioeconomic Pathway (SSP) scenarios were considered: SSP1– 2.6, SSP2– 4.5, and SSP5– 8.5 (low, intermediate, and high emissions, respectively) [86]. For each variable and analysis

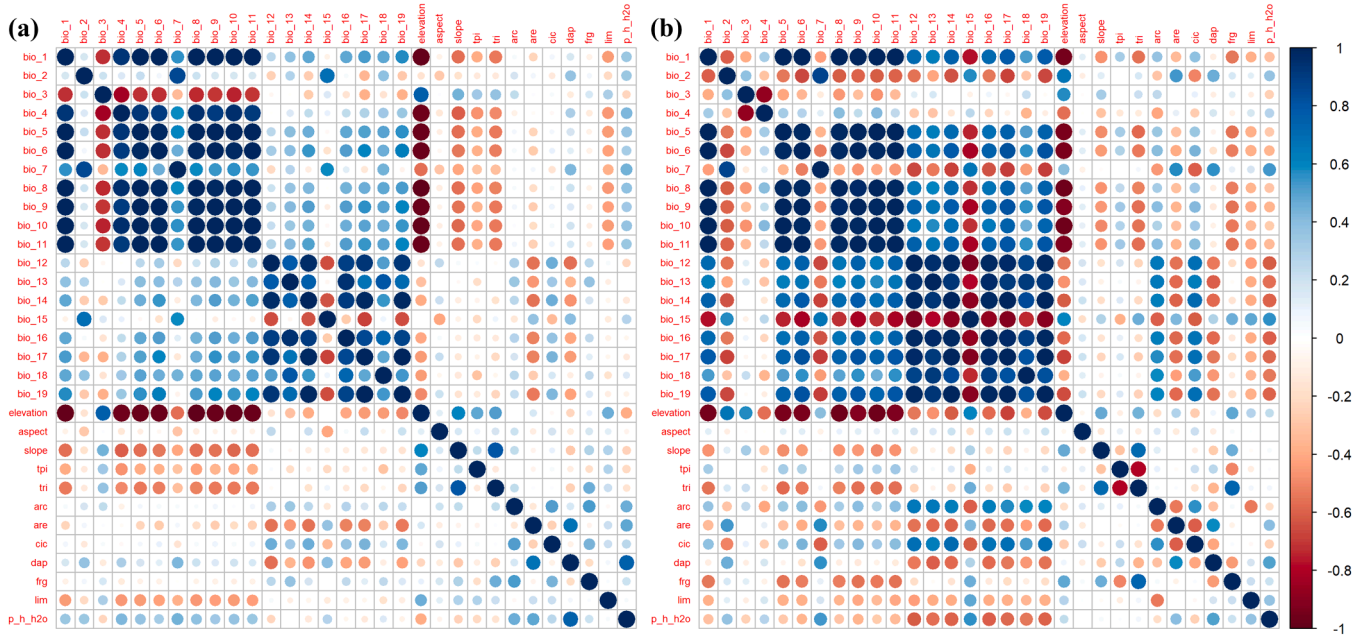

Fig. 3. Correlation analysis of environmental variables for plantain (a) and papaya (b).

period, projections were integrated using a multi-model ensemble based on the arithmetic mean of the two GCMs, an approach commonly used to increase robustness and reduce model-specific biases [87,88]. Projected changes were estimated for 2041–2060 and 2061–2080 (hereafter referred to as the 2050 and 2070 periods, respectively) using bioclimatic variables derived from monthly climate projections (maximum temperature, minimum temperature, and precipitation) from WorldClim v2.1. Because equivalent and consistent regional-scale projections are not available for all soil properties, and because topography does not vary over decadal timescales, edaphic and topographic variables were assumed to remain constant through time, a common assumption in regional assessments of future suitability.

2.8. Habitat suitability classification

The identification and delimitation of suitable areas for plantain and papaya crops were performed using a probability threshold that discriminates suitable and unsuitable areas. Several methods can be used to make this determination [37]. This study used the threshold based on TSS [76], which maximizes the sum of sensitivity and specificity [89]. Values above the threshold were classified as suitable habitats, and those below as unsuitable [90]. The potential distribution areas were reclassified into five levels of suitability: extremely suitable habitats ($P \geq 0.70$), moderately suitable habitats ($0.50 \leq P < 0.70$), low suitable habitats ($0.30 \leq P < 0.50$), unsuitable habitats ($0.10 \leq P < 0.30$) and extremely unsuitable ($P < 0.10$) [69,91,92]. This methodology facilitated the comparative visualization of areas with greater suitability under current and future projected climatic conditions, thus providing strategic information for agroclimatic planning and decision-making in the regional context.

2.9. Changes in the distribution pattern

The suitability surface was converted into binary files of suitable and unsuitable areas using the TSS threshold [76]. Then, the current distribution was superimposed onto each future scenario [93] to classify the spatial dynamics into exclusive categories that allow visualizing expansion, contraction, and persistence (no change). Additionally, within the zones that preserved their status, changes in the level of suitability were identified, distinguishing increased level and decreased level as redistribution patterns.

3. Results

3.1. Mapped environmental variables for the cultivation of plantain and papaya

The 31 environmental variables used to model plantain and papaya suitability are presented in Fig. 4, grouped into bioclimatic (a–s), topographic (t–x), and edaphic (y–ae) layers. Taken together, these variables reveal strong environmental heterogeneity across the study area. The main contrasts are associated with elevation, temperature, precipitation, and terrain configuration, which structure a marked lowland–upland gradient and define differentiated agroclimatic zones. In general, the central–eastern valleys and piedmont sectors exhibit warmer and less rugged conditions for crop establishment, whereas northern and higher-elevation areas show cooler and more heterogeneous conditions. Although edaphic variables are spatially less contrasted than climatic and topographic layers, they still show relevant variation in texture, cation exchange capacity, pH, and bulk density.

3.2. Performance of the species distribution models

The models showed high discriminative capacity for both crops under current and future conditions (Table 2). Under the current climate, the AUC reached 0.922 for plantain and 0.928 for papaya, indicating excellent predictive performance in both cases. In future projections, model performance remained consistently high, with very narrow variation across periods and scenarios. For plantain, AUC values ranged from 0.957 to 0.959, whereas for papaya they ranged from 0.963 to 0.965, confirming stable model behavior under all evaluated conditions.

In comparative terms, papaya consistently showed slightly higher AUC values than plantain, both under baseline conditions and across projected scenarios. Although the differences were small, this pattern was maintained across all evaluated scenarios. Likewise, the limited variation in AUC among SSP1– 2.6, SSP2– 4.5, and SSP5– 8.5 indicates that model predictive capacity was not substantially affected by the different future climate trajectories considered. Overall, model performance remained high across, periods, and scenarios

3.3. Contribution of environmental variables

The evaluation of the contribution of environmental variables in the potential distribution models of plantain and papaya showed differentiated patterns in the relative importance of bioclimatic, topographic, and edaphic factors (Fig. 5a and b).

In plantain, the variables with the greatest influence were elevation (58.97%), precipitation of the coldest quarter (Bio19; 13.39%), annual temperature range (Bio7; 8.47%), and silt content (7.55%). Together these variables accounted for >88% of the total model contribution. Additional variables such as precipitation of the warmest quarter (Bio18; 3.98%), aspect (1.65%), and coarse fragment content (0.99%) showed secondary contributions.

In papaya, the potential distribution revealed a strong dominance of temperature seasonality (Bio4), which explained 82.06% of the total contribution. This was followed, at a considerable distance, by precipitation of the warmest quarter (Bio18; 5.75%) and slope (2.18%). Other factors, such as soil pH (1.69%), bulk density (1.04%), and coarse fragment content (0.71%), presented smaller but relevant contributions.

Regarding permutation importance (Fig. 5c and d), in plantain the variables with the highest values were silt content (24.99%), annual temperature range (Bio7; 20.20%), and elevation (20.06%), indicating high sensitivity of the model to these variables. In papaya, temperature seasonality (Bio4; 71.81%) stood out as the dominant variable in permutation importance, followed by the topographic position index (9.41%) and the annual temperature range (3.70%).

3.4. Optimal environmental intervals

The ranges and mean values of the environmental variables that condition the potential distribution of plantain and papaya (Tables 3 and 4) were estimated using Youden's criterion (maximum sensitivity + specificity) to select the optimal cutoff point of the model. The response curves for the key environmental variables, derived from the MaxEnt models, are presented in the Appendix as Figs. A.1 and A.2 for plantain and papaya, respectively, providing a visual representation of the species-environment relationships and supporting the optimal intervals identified in Tables 3 and 4.

The optimal thresholds were 0.32 for plantain and 0.32 for papaya. From these thresholds, stricter and more permissive operational categories were defined, adjusting the cutoff point by 30% and 50% to identify, respectively, suitable and optimal conditions.

For plantain, the optimal intervals included edaphic, topographic, and climatic variables. Clay content presented an optimal range from 22.86 to 38.13% (mean: 32.20%), sand content ranged between 28.78 and 46.03% (mean: 40.31%), and silt content between 17.99 and 29.55% (mean: 26.15%). The cation exchange capacity varied from 20.04 to 35.11 cmol(+)/kg, with a mean value of 27.66 cmol(+)/kg, whereas soil pH ranged between 4.45 and 6.52, with a mean of 5.88. Topographically, the optimal areas were located at elevations from 367 to 1256 m a.s.l. (mean: 647.87 m), with a topographic position index of

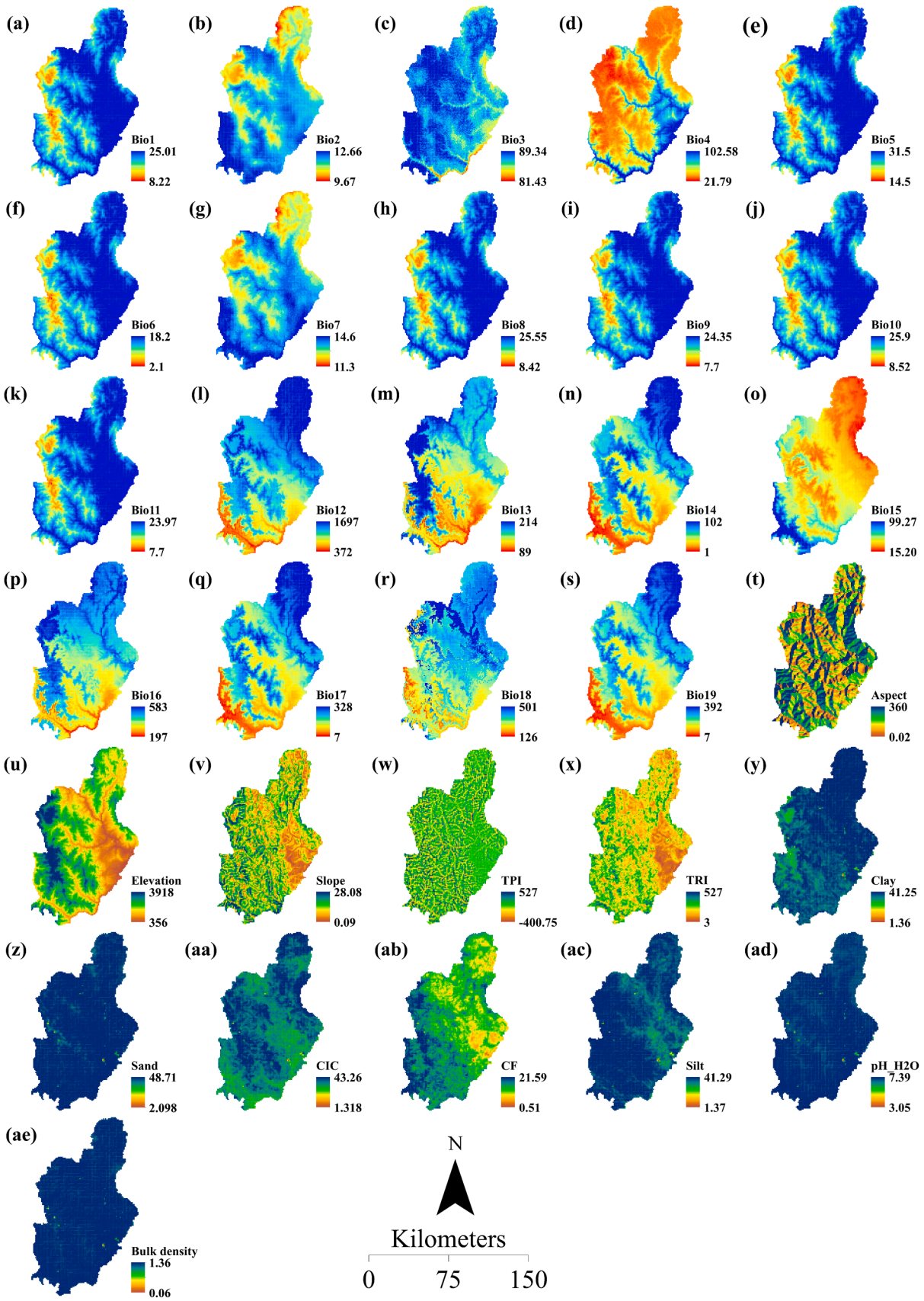

Fig. 4. Environmental variables mapped to determine the suitability of the provinces of Jaén and San Ignacio for plantain and papaya crops. For detailed information, refer to Table 1.

Table 2
Performance (AUC) of the distribution models of plantain and papaya under current climate and SSP scenarios (2050/2070) in northwestern Peru.

Period	Scenario	Plantain	Papaya
Current		0.922	0.928
2050	SSP1–2.6	0.957	0.963
	SSP2–4.5	0.958	0.965
	SSP5–8.5	0.958	0.964
2070	SSP1–2.6	0.958	0.963
	SSP2–4.5	0.957	0.964
	SSP5–8.5	0.959	0.965
Overall mean		0.953	0.959

–35.61 and a mean terrain ruggedness index of 87.77. Regarding climatic variables, precipitations from 274 to 460 mm were recorded during the warmest quarter (mean: 362.54 mm) and from 143 to 289 mm in the coldest quarter (mean: 225.12 mm), together with precipitation seasonality from 26.02 to 49.73% (mean: 30.92%). Annual temperature range presented a narrow range from 12.80 to 13.80 °C, with a mean of 13.31 °C.

For papaya, the optimal intervals also included edaphic variables. Clay content ranged between 25.79 and 38.42% (mean: 31.40%), sand content between 36.14 and 47.08% (mean: 41.50%), and silt content between 22.12 and 36.67% (mean: 26.46%). Bulk density varied between 1.04 and 1.35 g/cm³ (mean: 1.21 g/cm³), whereas coarse

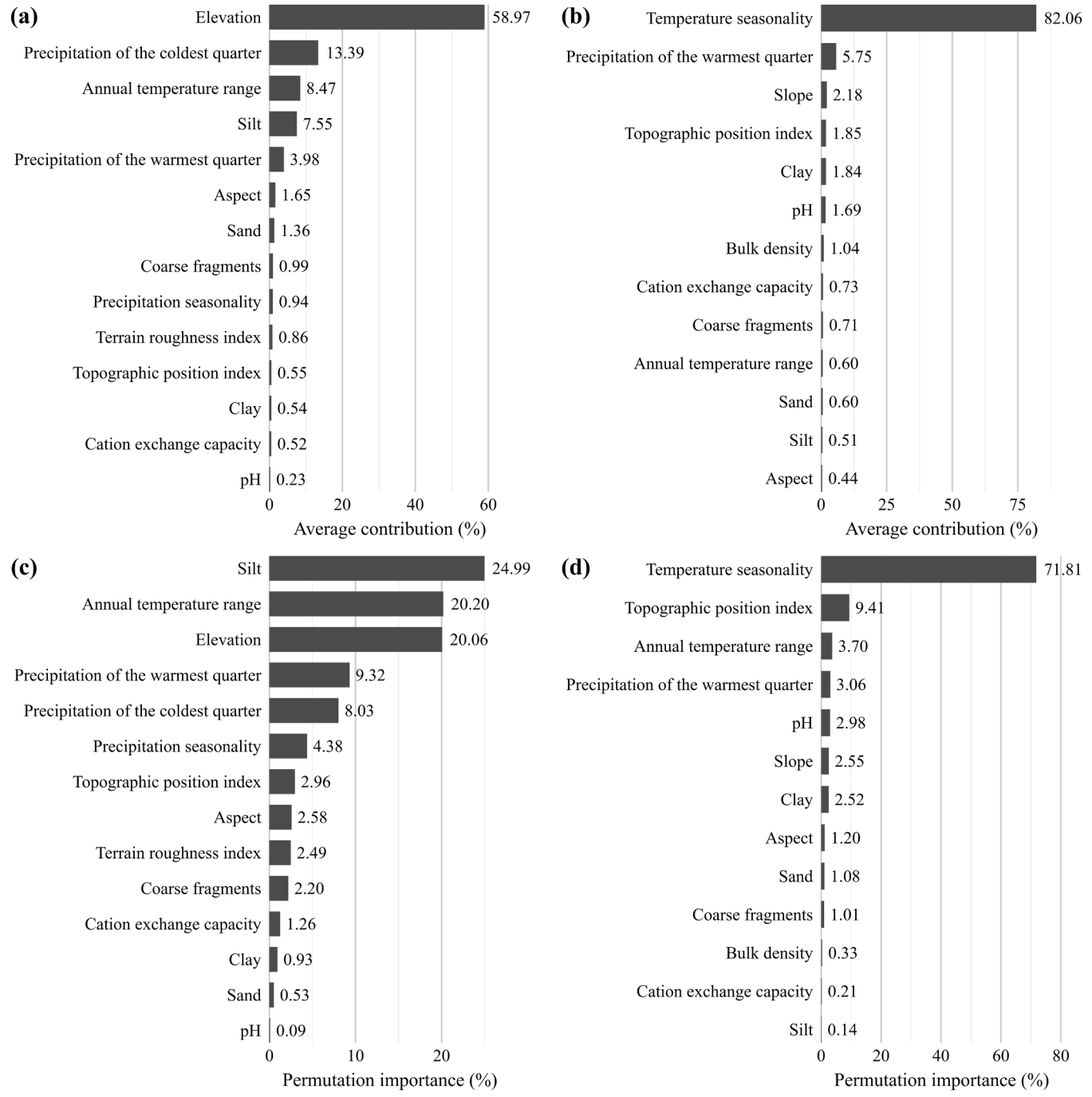

Fig. 5. Mean contribution and permutation of environmental variables in the MaxEnt models for plantain and papaya. (a) and (b) show the mean contribution (%) of the environmental variables to the potential distribution model of both crops, respectively. (c) and (d) represent the permutation importance (%) of the same variables.

Table 3
Ranges and means of the environmental variables under suitability index cutoff points (SI ≥ 30% and SI ≥ 50%) for plantain, defined from the optimal threshold determined with Youden's criterion (*Youden's J statistic*).

Variable	SI > 30%		SI > 50%	
	Value range	Mean	Value range	Mean
Annual temperature range (BIO5–BIO6)	12.80 - 13.80	13.31	12.80 - 13.80	13.31
Precipitation seasonality (coefficient of variation)	25.84 – 50.96	31.35	26.02 - 49.73	30.92
Precipitation of the warmest quarter	274 – 461	361.48	274 - 460	362.54
Precipitation of the coldest quarter	121 – 289	217.40	143 - 289	225.12
Elevation	365 – 1406	696.07	367 - 1256	647.87
Aspect	0.53 - 358.88	186.59	0.53 - 358.53	196.01
Topographic position index	−250.13 - 170.25	−28.38	−250.13 - 127.13	−35.61
Terrain ruggedness index	7.13 - 250.13	91.41	7.13 - 250.13	87.77
Cation exchange capacity of the topsoil layer	19.21 – 35.11	27.44	20.04 - 35.11	27.66
Clay content in the topsoil layer	22.50 – 38.42	32.25	22.86 - 38.13	32.20
Sand content in the topsoil layer	28.27 – 46.57	40.44	28.78 - 46.03	40.31
Silt content in the topsoil layer	17.76 – 30.03	26.30	17.99 - 29.55	26.15
Coarse fragment content in the topsoil layer	3.09 – 13.03	8.34	3.10 - 12.71	8.42
Measure of soil acidity or alkalinity, based on the concentration of H^+ ions	4.24 – 6.52	5.88	4.45 - 6.52	5.88

Table 4
Ranges and means of the environmental variables under suitability index cutoff points (SI ≥ 30% and SI ≥ 50%) for papaya, defined from the optimal threshold determined with Youden's criterion (*Youden's J statistic*).

Variable	SI > 30%		SI > 50%	
	Value range	Mean	Value range	Mean
Temperature seasonality (standard deviation ×100)	61.02 - 95.17	75.68	62.56 - 93.45	76.38
Annual temperature range (BIO5–BIO6)	13.00 - 14.20	13.45	13.10 - 14.10	13.44
Precipitation of the warmest quarter	192 – 458	345.42	207 – 458	355.76
Aspect	0.53 - 358.88	171.29	0.53 - 358.88	170.48
Slope	0.10 - 13.63	4.01	0.10 - 11.70	3.55
Topographic position index	−240.50 - 65.13	−52.38	−240.50 - 38.63	−55.22
Clay content in the topsoil layer	24.88 – 38.42	31.36	25.79 – 38.42	31.40
Sand content in the topsoil layer	35.41 – 47.07	41.37	36.14 – 47.08	41.50
Silt content in the topsoil layer	22.16 – 33.67	26.52	22.16 – 33.67	26.46
Reference bulk density of the topsoil layer	1.01 – 1.36	1.21	1.04 – 1.35	1.21
Coarse fragment content in the topsoil layer	3.00 – 15.19	8.19	3.00 – 14.39	7.84
Measure of soil acidity or alkalinity, based on the concentration of H^+ ions	5.16 - 7.05	6.04	5.17 – 6.79	6.02

fragment content was between 3 and 14.39% (mean: 7.84%). Soil pH presented a range from 5.17 to 6.79, with a mean of 6.02. Topographically, the optimal areas were associated with slopes between 0.10 and 11.70° (mean: 3.55°), a mean topographic position index of –55.22, and an aspect of 170.48° From a climatic point of view, precipitation during the warmest quarter varied between 207 and 458 mm (mean: 355.76 mm), whereas temperature seasonality (Bio4) ranged between 62.56 and 93.45 with a mean of 76.38. Annual temperature range presented a narrow interval from 13.10 to 14.10 °C, with a mean of 13.44 °C.

Taken together, both crops share a preference for climatic conditions with a very stable and similar annual temperature range (plantain: 13.31 °C; papaya: 13.44 °C). However, they are distinguished in other climatic aspects: papaya presents higher temperature seasonality (Bio4, mean 76.38), whereas for plantain suitability is more associated with precipitation seasonality (Bio15, mean 30.92%) and higher precipitations during the coldest quarter (225.12 mm). From a topographic perspective, both species are concentrated in concave topographic positions (TPI < 0), with this trait being more pronounced in papaya (–55.22 versus –35.61). In the edaphic component, optimal soils present a loam texture; papaya is associated with slightly higher contents of sand (41.50% versus 40.31%) and lower contents of clay (31.40% versus 32.20%) compared with plantain A notable contrast is the higher cation exchange capacity (CEC) associated with plantain optimal areas (27.66 cmol(+)/kg) compared to papaya.

3.5. Uncertainty in the model results

Fig. 6 depicts the predictive uncertainty of the models based on the standard deviation of predictions across 25 cross-validation folds (k = 25), rescaled to 0–100%. On the color scale, green tones indicate low uncertainty, whereas yellow-to-red tones reflect high uncertainty.

In plantain (Fig. 6a), low uncertainty predominates along the valley–piedmont corridor associated with the Chinchipe, Marañón, and Chamaya rivers, indicating high model stability in geomorphological units well represented by the data. The highest uncertainties are concentrated on mountain ridges and slopes and toward the boundaries of the study area, where strong topographic/environmental gradients coexist with lower data support.

In papaya (Fig. 6b) the pattern is more heterogeneous, with moderate–high uncertainty over the eastern slopes and the southeastern sector, especially outside the main valleys of the Chinchipe and the Marañón; in contrast, valley bottoms and local plains maintain low standard deviation values. This behavior suggests greater sensitivity of the papaya model to environmental gradients and to the spatial configuration of the sampling, in comparison with plantain.

In both models, high uncertainty aligns with environmental transition zones and peripheral sectors, whereas low uncertainty is concentrated in the main valleys (Chinchipe, Marañón and Chamaya), where the environmental space was better covered by the training replicates. Accordingly, projected changes located in the main valleys and the valley–piedmont corridor (low uncertainty) are interpreted with greater confidence, whereas transitions on slopes, peripheral sectors, and environmental transition zones (higher uncertainty) should be interpreted cautiously and prioritized for monitoring and adaptive planning (Fig. 6).

3.6. Current and future potential distribution areas of plantain and papaya

Percent changes in high suitability (extremely + moderately suitable) were calculated relative to the baseline high-suitability area (plantain: 818.79 km^2; papaya: 511.01 km^2), whereas the coverage of the extremely unsuitable class is expressed as a proportion of the total study area.

Currently, areas of high suitability for plantain (extremely + moderately suitable) cover 818.79 km^2, concentrated in the lowlands of the central–eastern corridor (367–1256 m a.s.l.). Under future scenarios, a progressive reduction of these areas is projected, together with an expansion of the extremely unsuitable class, particularly under high-

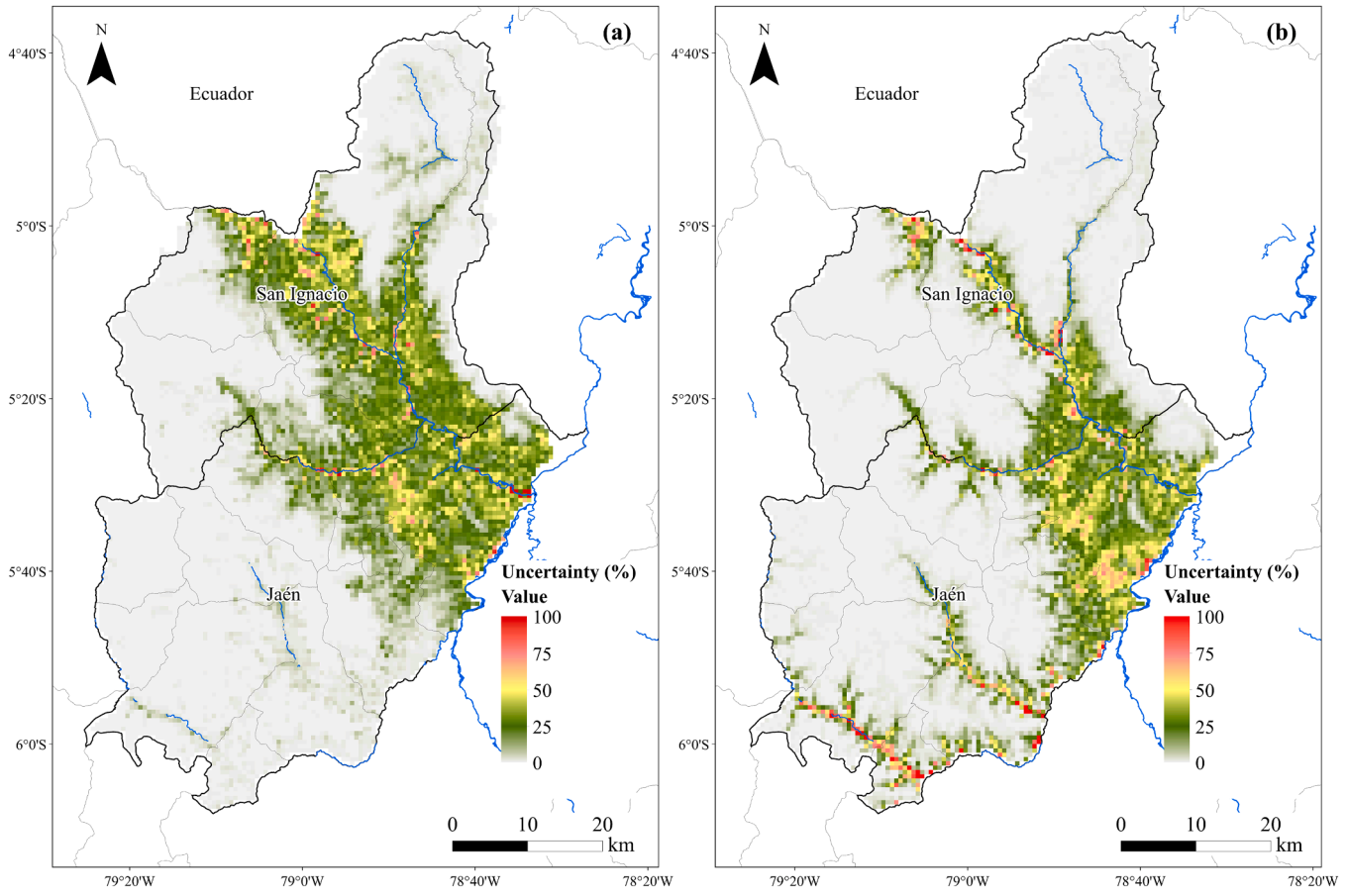

Fig. 6. Predictive uncertainty (normalized standard deviation, 0–100%) among cross-validation folds (k = 25) for plantain **(a)** and papaya **(b)**.

emission pathways and toward 2070 (Fig. 7, Table 5).

By 2050, high suitability deteriorates as emissions increase (Fig. 7b-d). Under the low-emission scenario (SSP1– 2.6), high suitability remains virtually stable (0.00%; 818.79 km^2), whereas under SSP2– 4.5 and SSP5– 8.5 net losses of −12.68% (714.94 km^2) and −25.68% (608.54 km^2) are projected, respectively, relative to the baseline (818.79 km^2). This pattern is mainly driven by contractions of the extremely suitable class under SSP2– 4.5 (−20.96%) and SSP5– 8.5 (−37.38%), which are not offset by gains in lower-suitability categories.

By 2070, the declining trend intensifies across all scenarios (Fig. 7e-g), with net losses of high suitability ranging from −17.99% (SSP1– 2.6; 671.51 km^2) to −42.35% (SSP5– 8.5; 472.01 km^2). The most severe contraction occurs under SSP5– 8.5, where extremely suitable areas decrease by −67.66% (from 373.64 km^2 to 120.85 km^2), while the extremely unsuitable class expands by +17.47%, reaching 8836.46 km^2, equivalent to 89.29% of the study area (Table 5). Even under the most optimistic scenario (SSP1– 2.6, 2070), extremely suitable areas decline by −31.43%, indicating a substantial loss of highly suitable habitat for plantain regardless of the emission pathway. Overall, the largest reductions in high suitability and the greatest expansion of extremely unsuitable area occurred under SSP5– 8.5 in 2070.

Current high-suitability areas for papaya (extremely + moderately suitable) total 511.01 km^2, also concentrated in the central–eastern corridor. In contrast to plantain, papaya exhibits a biphasic response: net gains in high suitability under low to high emissions by 2050, followed by net losses by 2070 across all scenarios, with particularly severe contractions under high emissions (Fig. 8; Table 6).

By 2050 (Fig. 8b-d), high-suitability areas increase under SSP1– 2.6 (+26.50%) and SSP5– 8.5 (+8.53%), while showing a slight reduction under SSP2– 4.5 (−5.07%). The extremely unsuitable class expands across all scenarios, with increases ranging from +6.47% to +12.29%.

By 2070, this polarization intensifies and net losses of high suitability prevail across all scenarios (Fig. 8e-g): −1.95% (SSP1– 2.6), −17.67% (SSP2– 4.5), and −34.59% (SSP5– 8.5). Under high emissions, extremely suitable areas contract by −35.40% (from 218.71 km^2 to 141.29 km^2), while the extremely unsuitable class reaches its maximum expansion (9390.72 km^2; +15.50%), equivalent to 91.17% of the study area (Table 6). By 2070, net losses of high suitability and expansion of the extremely unsuitable class prevail across all scenarios, with the most pronounced changes occurring under SSP5– 8.5

3.7. Changes in spatial patterns in the future

The comparison between current climatic conditions and the projections for 2050 and 2070 under SSP1– 2.6, SSP2– 4.5, and SSP5– 8.5 shows spatial patterns of suitability for plantain. Across scenarios, corridors of suitability gain (expansion + increased level) are identified along the central–eastern axis, whereas losses (decreased level + contraction) are predominantly concentrated toward the north and higher-elevation sectors, intensifying under high emissions toward 2070 (Fig. 9; Table 7). Quantitatively, unchanged areas dominate the territory (78.93–85.92%); however, the net balance (gains minus losses) is consistently negative. For 2050, gains account for 1.27–3.31%, while losses reach 10.78–16.10%, resulting in net losses ranging from −710.48 km^2 (−7.47%) to −1410.16 km^2 (−14.82%). By 2070, net losses increase to −1341.21 km^2 (−14.09%) and −1690.87 km^2 (−17.77%), with the most critical conditions projected under SSP5– 8.5, which combines the greatest contraction (415.38 km^2) and the largest decrease in suitability level (1432.58 km^2) (Table 7; Fig. 9). Spatially, the central–eastern gain corridors remain identifiable; however, the area affected by losses exceeded the area affected by gains in all scenarios.

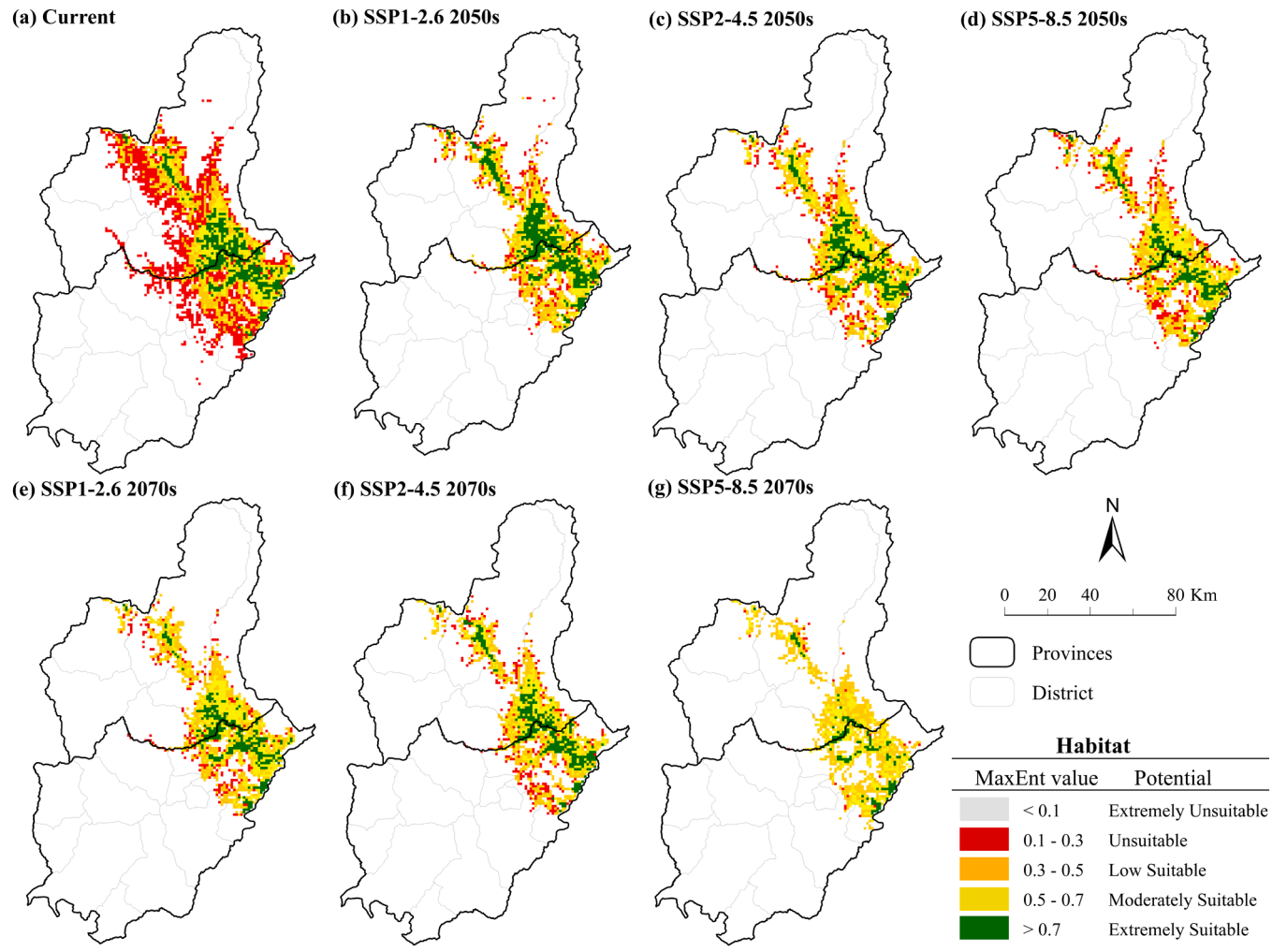

Fig. 7. Current distribution and future projection of the climatic suitability of plantain under three climate scenarios (SSP1– 2.6, SSP2– 4.5 and SSP5– 8.5) for the periods 2050 and 2070.

Table 5
Dynamic changes of suitable areas of plantain (km^2) under different climate scenarios.

Period	Scenario	Extremely Suitable	Change (%)	Moderately Suitable	Change (%)	Low Suitable	Change (%)	Unsuitable	Change (%)	Extremely Unsuitable	Change (%)
Current	Current	373.64		445.15		528.59		1027.04		7522.18	
2050	SSP1–2.6	426.41	14.12	392.38	−11.86	539.62	2.09	229.81	−77.62	8308.37	10.45
	SSP2–4.5	295.33	−20.96	419.61	−5.74	500.49	−5.32	210.24	−79.53	8470.91	12.61
	SSP5–8.5	234.04	−37.36	374.50	−15.87	541.33	2.41	257.04	−74.97	8489.69	12.86
2070	SSP1–2.6	256.17	−31.44	415.34	−6.70	534.54	1.13	175.34	−82.93	8515.21	13.20
	SSP2–4.5	274.06	−26.65	343.87	−22.75	463.88	−12.24	205.12	−80.03	8609.67	14.46
	SSP5–8.5	120.85	−67.66	351.16	−21.12	565.15	6.92	22.98	−97.76	8836.46	17.47

For papaya, unchanged areas also dominate (84.44–89.84%), but losses again exceed gains across all scenarios and periods (Table 8; Fig. 10). Spatially, gains (expansion + increased level) are located predominantly along the central–eastern axis, whereas losses (contraction + decreased level) are concentrated mainly toward the southern and western portions of the study area. Quantitatively, in 2050 gains range from 0.85% (80.84 km^2) to 4.41% (419.53 km^2), while losses reach 5.94–11.15% (565.49–1061.27 km^2), yielding negative net balances from −145.96 km^2 (−1.53%) to −888.54 km^2 (−9.34%) (Table 8; Fig. 10). By 2070, the net balance becomes more negative and ranges from −893.95 km^2 (−9.40%) to −1419.63 km^2 (−14.92%), with the most critical case under SSP5– 8.5 (Table 8; Fig. 10). Under this scenario, the highest absolute values of decreased level (1261.52 km^2) and contraction (188.74 km^2) are also observed.

In both crops, most of the territory remained in the same suitability class, but gain areas were spatially localized and consistently smaller than loss areas, resulting in negative net balances that were strongest under higher-emission scenarios and in 2070. The proportions of

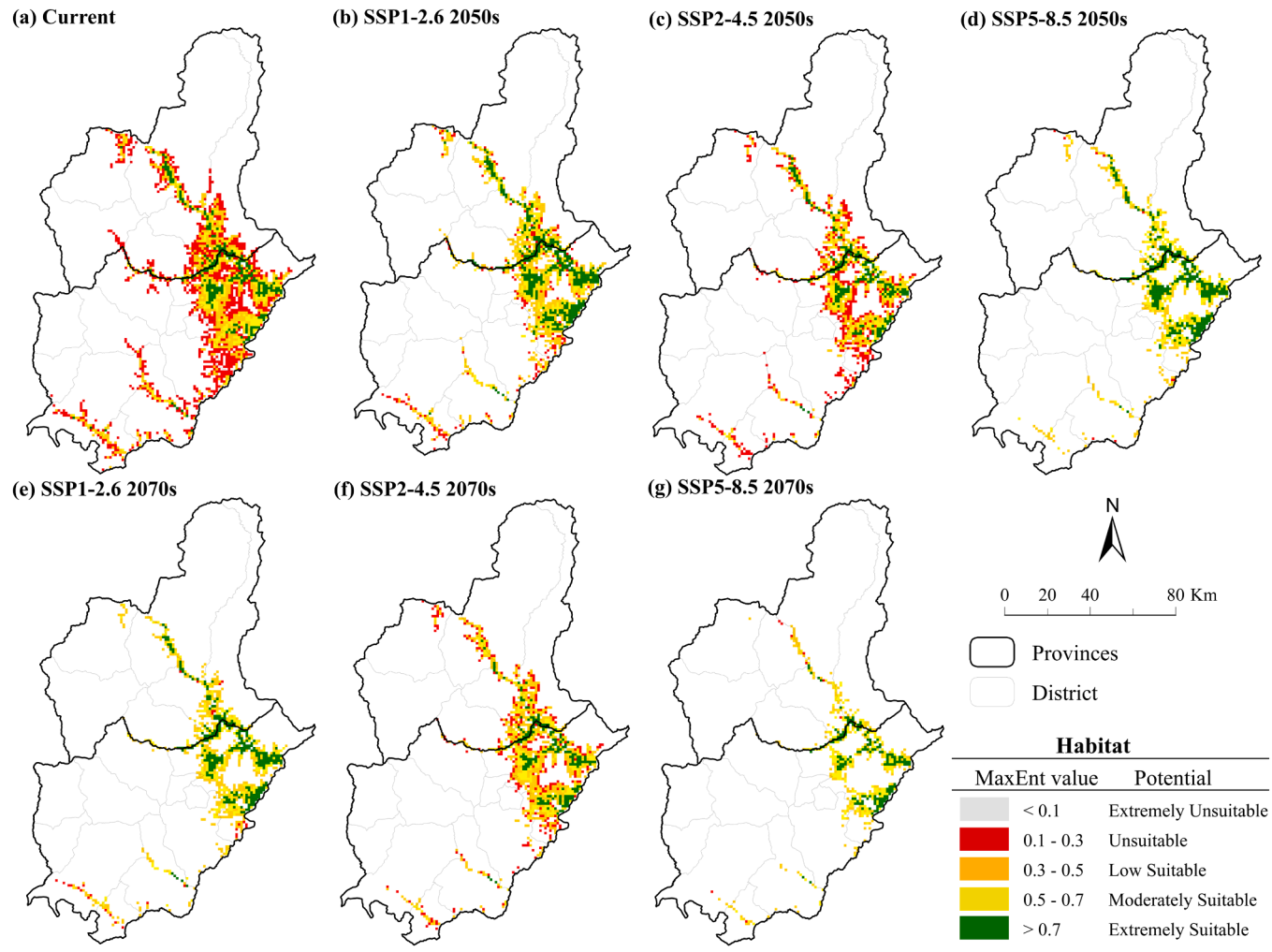

Fig. 8. Current distribution and future projection of the climatic suitability of papaya under three climate scenarios (SSP1– 2.6, SSP2– 4.5 and SSP5– 8.5) for the periods 2050 and 2070.

Table 6
Dynamic changes in suitable areas of papaya under different climate scenarios.

Period	Scenario	Extremely Suitable	Change (%)	Moderately Suitable	Change (%)	Low Suitable	Change (%)	Unsuitable	Change (%)	Extremely Unsuitable	Change (%)
Current	Current	218.71		292.30		471.98		781.01		8132.60	
2050	SSP1–2.6	353.16	61.47	293.35	0.36	447.98	−5.08	141.24	−81.92	8660.87	6.50
	SSP2–4.5	224.67	2.72	260.21	−10.98	423.25	−10.32	113.16	−85.51	8875.30	9.13
	SSP5–8.5	285.93	30.73	268.77	−8.05	203.15	−56.96	7.54	−99.04	9131.20	12.28
2070	SSP1–2.6	252.74	15.56	248.29	−15.06	329.66	−30.15	24.67	−96.84	9041.24	11.17
	SSP2–4.5	165.94	−24.13	250.00	−14.47	419.91	−11.03	235.67	−69.82	8825.07	8.51
	SSP5–8.5	141.26	−35.41	192.92	−34.00	164.04	−65.24	7.66	−99.02	9390.72	15.47

expansion, contraction, increased/decreased level, and unchanged areas are presented in Tables 7–8.

4. Discussion

The projected redistribution of suitability for plantain and papaya indicates that climate change is likely to reconfigure the agricultural territory unevenly, generating localized areas of gain that, in general terms, do not offset the prevailing trend of suitability deterioration at the regional scale. This pattern is consistent with previous studies showing that the impacts of climate change on crop suitability are not distributed uniformly, but rather vary according to the production system, biophysical conditions, and location, with implications for production, food security, and rural livelihoods [94,95]. In this context, the consistently high predictive performance of the models supports the robustness of the spatial inferences and reinforces the usefulness of these projections for informing adaptation decisions and territorial prioritization. From this perspective, suitability modeling has been recognized

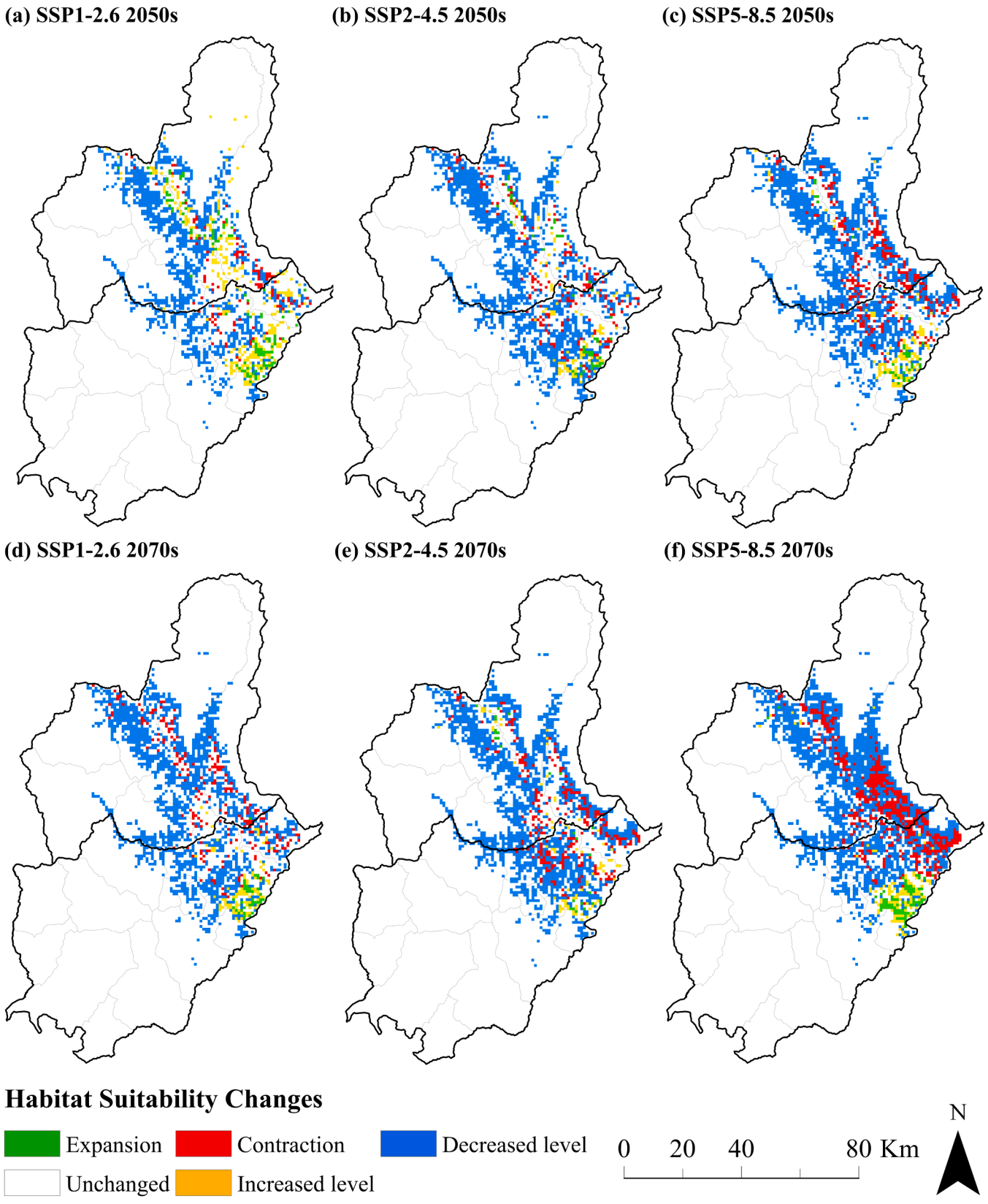

Fig. 9. Changes in habitat suitability for plantain from the current climate (baseline) towards the periods 2050 and 2070 under the SSP1– 2.6, SSP2– 4.5 and SSP5– 8.5 scenarios.

Table 7
Dynamic changes in suitable areas of plantain under SSP1– 2.6, SSP2– 4.5 and SSP5– 8.5 scenarios in 2050 and 2070.

Period	Scenario	Area (km^2)				
		Expansion	Unchanged	Contraction	Increased Level	Decreased Level
2050s	SSP2.6	95.32	8176.35	95.33	219.58	930.05
	SSP4.5	42.55	8056.36	146.40	78.29	1193.02
	SSP8.5	29.78	7863.12	240.03	91.89	1291.80
2070s	SSP2.6	32.33	7954.20	179.61	78.28	1272.21
	SSP4.5	22.98	7872.50	223.85	65.53	1331.77
	SSP8.5	68.60	7511.58	415.38	88.49	1432.58

Table 8
Dynamic changes in suitable areas of papaya under SSP1– 2.6, SSP2– 4.5 and SSP5– 8.5 scenarios in 2050 and 2070.

Period	Scenario	Area (km^2)				
		Expansion	Unchanged	Contraction	Increased Level	Decreased Level
2050s	SSP1–2.6	148.07	8529.61	12.57	271.46	552.92
	SSP2–4.5	28.93	8547.55	55.07	51.91	831.19
	SSP5–8.5	87.64	8280.63	43.95	85.09	1017.32
2070s	SSP1–2.6	37.44	8423.29	47.42	61.26	945.23
	SSP2–4.5	18.72	8480.37	113.79	31.48	870.28
	SSP5–8.5	11.91	8033.76	188.74	18.72	1261.52

as a source of spatially explicit information to support decisions on research, investment, and adaptation, while also highlighting that recommendations must be locally tailored and should avoid generalized or uniform approaches [96,97]. Taken together, these findings underscore the need for evidence-based adaptation strategies and for the informed prioritization of cropping areas [94,95].

The integration of bioclimatic predictors with edaphic and topographic layers in MaxEnt made it possible to reconstruct suitability patterns consistent with the ecophysiology of both crops and, at the same time, to evidence transitions dominated by level drops as the forcing increases. According to [31], this approach reduces biases of exclusively climatic models by incorporating local soil and relief conditioning factors. In plantain, suitability is concentrated in valley–piedmont corridors, but the drop in suitability level systematically exceeds the gains. Thermo-hydric mismatches, together with edaphic and topographic limitations, degrade suitability rather than inducing spatial contractions—suggesting that suitability deterioration is associated with combined thermo-hydric, edaphic, and topographic constraints; this is consistent with the high water demand and deep soils required by the root system [93]. In papaya, although some scenarios show temporary gains, the balance becomes negative towards 2070, indicating that this initial climatic advantage is insufficient to counteract the cumulative effects of thermal stress and the progressive expansion of climatically unsuitable areas under warmer scenarios [98].

The analysis of contribution and permutation importance confirms differentiated ecophysiological fundamentals between crops [33,99]. In plantain, elevation, precipitation during the coldest quarter, annual temperature range, and silt content stand out, together explaining >88% of the contribution (Fig. 5a) and demonstrating the co-dependence of altitudinal gradients, water regime, and edaphic properties. In the permutation, the highest values correspond to silt, annual temperature range and elevation (Fig. 5c), reinforcing their role as key predictors. These variables not only delineate the current ecological niche of the species, but will constitute the main determinants of its potential distribution towards the future [100], defining a niche dependent on stable thermo-hydric conditions and soils with good moisture retention, which is consistent with its high sensitivity to prolonged water deficits [93,101]. In papaya, temperature seasonality predominates (Fig. 5b and d), which indicates a critical dependence on intra-annual thermal variability, which is determinant for sensitive phenological processes such as flowering and fruit set [102] and with its vulnerability to excess water or prolonged droughts, conditions that affect germination, growth, and productivity [98].

The characterization of the optimal environmental intervals for plantain and papaya translates the model results into quantitative parameters applicable in the field, finding a solid correspondence with the key predictors identified. For plantain, the optimal altitudinal range (367–1256 m a.s.l.) and the narrow annual temperature range (12.80–13.80 °C) are consistent with the restricted optimal interval detected for elevation and annual temperature range, suggesting sensitivity to thermal variability and seasonal moisture conditions [21]. This relationship underscores the crop's adaptation to very stable thermal and moisture conditions, explaining its concentration at specific altitudes. Likewise, the need for deep soils with high silt content and Cation Exchange Capacity (CEC), which reflects its requirement for buffering against drought [93], is supported by the positive influence of soil organic carbon and bulk density [93,103,104]. These physicochemical factors are critical for the availability of water and nutrients, necessary to support the extensive root system reported in agronomic literature [104,105], where a reduction in bulk density can improve soil structure and growth [106].

Papaya showed a wider optimal window in slope (0.10–11.70°) and a slightly less acidic pH (pH 5.17–6.79), which indicates greater edaphic plasticity. However, its extreme sensitivity is confirmed within the range of temperature seasonality (Bio4: 62.56–93.45), a crucial threshold for bloom failure risk management. This finding is consistent with previous studies that report that temperatures outside the range of 10–35 °C cause disorders in floral and fruit development [107,108], while optimal germination occurs between 29.5 and 30 °C [109,110]. These results indicate that, although papaya may show temporary gains in suitability under some 2050 scenarios, this advantage is not sustained over time. By 2070, suitability declines across all scenarios, particularly under SSP5– 8.5, where extremely suitable areas contract and extremely unsuitable areas reach their maximum extent, reinforcing the need for irrigation and drainage management to buffer increasing thermal and water stress. These quantitative intervals not only validate our model

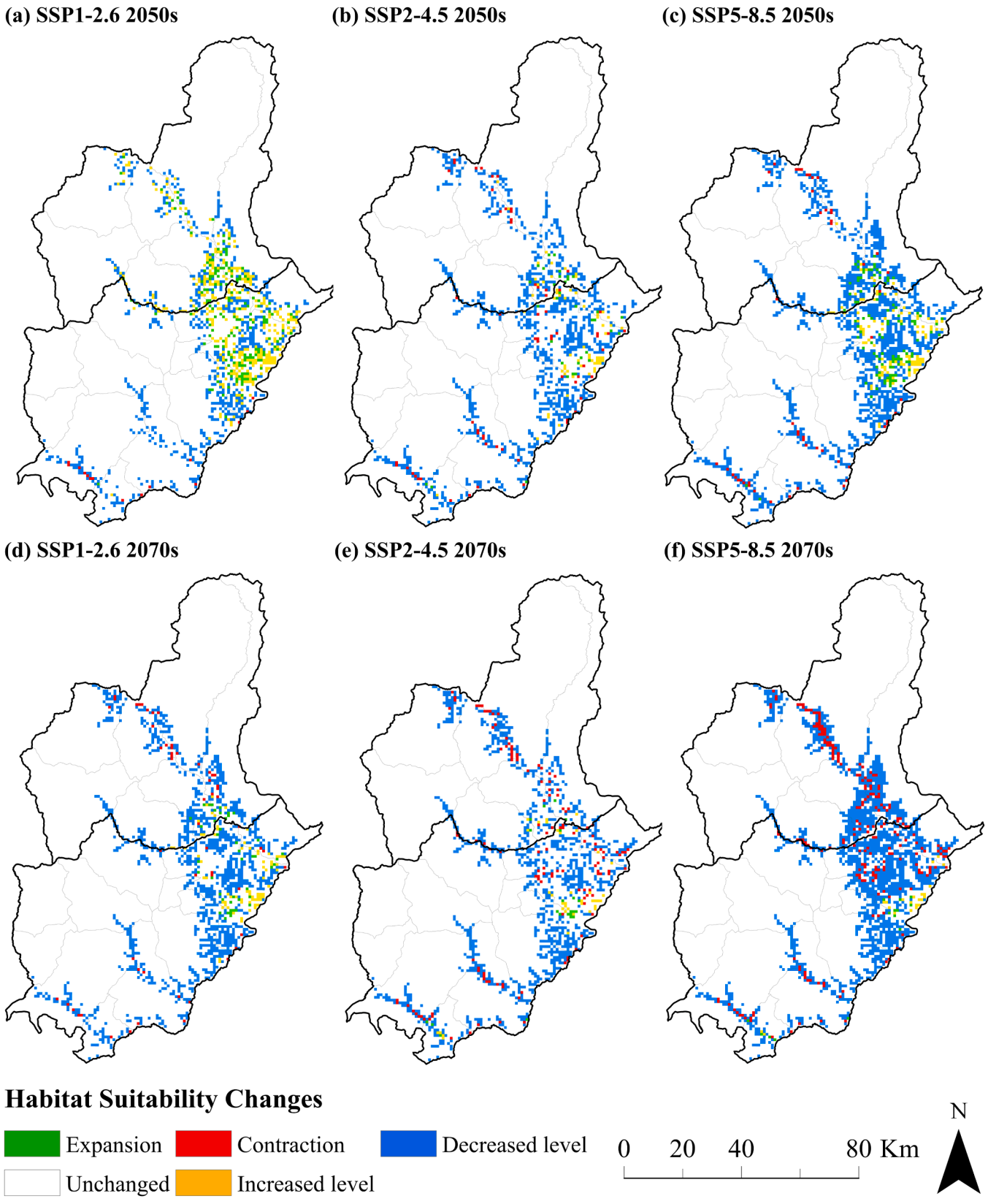

Fig. 10. Changes in habitat suitability for papaya from the current climate (baseline) towards the periods 2050 and 2070 under the SSP1– 2.6, SSP2– 4.5 and SSP5– 8.5 scenarios.

against established agronomic knowledge, but also provide specific technical criteria for site selection, soil management, and irrigation, allowing for the adjustment of management practices to maximize the potential productivity of papaya in the region under a changing climate.

The projection of spatial changes under different SSP scenarios reveals that, on a territorial scale, the net suitability balance is negative for both crops. For plantain, the most critical spatial pattern was projected under SSP5– 8.5 in 2070, where the combined effect of contraction (415.38 km^2) and decreased suitability level (1432.58 km^2) resulted in the largest net loss (−1690.87 km^2). This indicates that the deterioration of suitability occurs not only through spatial retreat, but also through downgrading within areas that remain climatically occupied [111,112]. For papaya, the net balances were also consistently negative, reaching −1419.63 km^2 in the same critical scenario. The projected gains for this crop (expansion + increased level) were modest in all cases, with a maximum of 419.53 km^2 (SSP1– 2.6, 2050), being insufficient to counteract the extensive losses.

The concentration of these limited gains in the valleys of the Chinchipe, Marañón, and Chamaya rivers for both crops suggests a decisive shelter effect mediated by the terrain [113,114], a finding consistent with impact mitigation in areas of high topographic heterogeneity [96]. This pattern of widespread net losses, with insufficient and concentrated gains, supports warnings about the risks of relying on a single global model as it ignores heterogeneities [115]. Consequently, information with fine spatial resolution is indispensable for regional analysis; otherwise, areas where climate change aggravates conditions could be overlooked, which demands adaptation measures focused per crop [116].

The low uncertainty in the valley bottoms, where stable areas and projected gains overlap, provides greater relative confidence for identifying these corridors as priority areas for further evaluation and adaptation planning. On the contrary, the moderate to high uncertainty on slopes and peripheral areas, more pronounced for the papaya model, reflects the sensitivity of MaxEnt to abrupt environmental gradients and a lower density of training data in these zones [37,117]. This pattern does not invalidate the loss projections in these areas but suggests they should be treated with caution and prioritizing in them adaptive management strategies and continuous monitoring programs, in line with robust risk management approaches in the face of climate uncertainty [117,118].

The consistency of the results obtained with studies conducted in other tropical regions confirms the robustness of the MaxEnt framework in the assessment of climate impacts on fruit crops [31,32,93,119]. The application of two CMIP6 GCMs and three socioeconomic pathways (SSP1– 2.6, SSP2– 4.5 and SSP5– 8.5) helps to explore scenario-related uncertainty and provides a comprehensive overview for regional agricultural planning. In global terms, this work contributes to the growing evidence that tropical fruit trees not only face risks from climate change, but can also experience expansion opportunities into new areas, provided that timely adaptation policies are implemented [32,96,98].

This study should be interpreted in light of the structural limitations inherent to climate–environmental suitability modeling. Although incorporating edaphic and topographic predictors can reduce part of the bias associated with purely climate-based approaches in heterogeneous landscapes, the model estimates potential suitability rather than realized agronomic performance; therefore, projected suitability classes should not be interpreted as direct indicators of yield, profitability, or effective land availability [27,63]. In real agricultural systems, crop presence and persistence are also shaped by management practices (e.g., irrigation and drainage), varietal selection, pest and disease pressure, market accessibility, and land tenure—factors that were not explicitly represented in this analysis [27].

Additional uncertainty is associated with the calibration data, future projections, and the inherent scope of the modeling approach. Occurrence records compiled from multiple sources were spatially filtered at 1 km to reduce clustering and spatial autocorrelation, although residual sampling bias may persist in densely sampled areas [52,53]; likewise, pseudo-absences provide an operational environmental contrast rather than verified crop absence [50]. Future projections also depend on the selected GCMs and on assumptions regarding predictor stability: edaphic and topographic variables were assumed to remain constant through time, and thus potential changes related to soil degradation, erosion, or conservation practices are not captured [120]. Although the arithmetic ensemble of two GCMs improves robustness, it does not represent the full range of climatic uncertainty, particularly for precipitation in tropical Andean environments [88,121]. Finally, the 1-km spatial resolution may smooth fine-scale topographic and environmental gradients, and extrapolation to potentially novel climatic conditions warrants caution, especially in transition zones and under high-emission scenarios [122].

Despite these limitations, the modeling framework provides a robust basis for regional-scale inference and offers spatially explicit evidence that is relevant for adaptation planning, territorial prioritization, and climate-risk management for plantain and papaya in northwestern Peru. Future research should integrate environmental suitability models with crop models to better translate climatic potential into expected agronomic performance under contrasting management conditions. It would also be valuable to simulate adaptive scenarios involving irrigation and drainage improvements, increased water-use efficiency, and the use of stress-tolerant planting material, as well as to extend validation to other production zones and environmentally heterogeneous landscapes. Such efforts would help assess the transferability of the present framework and support the development of more robust, site-specific strategies for climate adaptation and sustainable agricultural planning in northwestern Peru.

5. Conclusions

The current and future suitability of plantain and papaya in Jaén and San Ignacio was modeled under SSP1– 2.6, SSP2– 4.5, and SSP5– 8.5, using models with high predictive performance (current AUC = 0.922–0.928; projected AUC = 0.957–0.965). Although a large proportion of the territory remained in the same suitability category (78.93–89.84%, depending on crop, scenario, and period), this apparent stability masks a critical spatial redistribution for agricultural production. For plantain, gain corridors located mainly along the central–eastern axis do not offset the losses associated with decreased suitability level and contraction toward higher and more marginal areas, with the most severe net loss projected under SSP5– 8.5 in 2070. For papaya, some short-term gains in high-suitability areas are projected by 2050, but by 2070 net losses predominate across all scenarios, accompanied by a marked expansion of extremely unsuitable areas (reaching 91.17% of the study area under SSP5– 8.5 in 2070).

These patterns reflect differentiated ecophysiological controls: plantain suitability is mainly associated with elevation, precipitation of the coldest quarter, and silt content, whereas papaya suitability is strongly constrained by temperature seasonality. Overall, the results indicate that the vulnerability of currently suitable areas outweighs the opportunities for future expansion. Therefore, adaptation strategies should prioritize the central–eastern corridors, strengthen water management, and guide territorial planning toward the most climatically resilient production areas.

Ethical statement

This study did not involve human participants or experimental animals and therefore did not require approval by an institutional ethics committee. All remote sensing and environmental data were obtained from public or institutional sources and used in accordance with their terms of use. No personal or sensitive information is included in this research.

Funding

This work was supported by the Instituto Nacional de Innovación Agraria (INIA) through the Investment Project with CUI N° 2472,675 titled: "Mejoramiento de los servicios de investigación y transferencia de tecnología agraria en la estación agraria experimental Baños del Inca en la localidad de Baños del Inca del distrito de Baños del Inca – provincia de Cajamarca - departamento de Cajamarca.

Declaration of generative AI and AI-assisted technologies in the manuscript preparation process

During the preparation of this work the author used Chat GPT in order to improve readability and language. After using this tool, the authors reviewed and edited the content as needed and take full responsibility for the content of the publication.

CRediT authorship contribution statement

Jefferson A. Cubas Sanchez: Writing – original draft, Validation, Software, Methodology, Investigation, Formal analysis, Data curation, Conceptualization. **Beimer Chuquibala-Checan:** Writing – review & editing, Validation, Formal analysis, Data curation. **Nilton Atalaya-Marin:** Writing – review & editing, Validation, Formal analysis, Data curation. **Daniel Tineo:** Writing – review & editing, Visualization, Project administration, Funding acquisition. **Victor H. Taboada-Mitma:** Visualization, Validation, Supervision, Project administration, Funding acquisition. **Héctor Cabrera-Hoyos:** Visualization, Validation, Supervision, Data curation. **Juancarlos Cruz-Luis:** Validation, Supervision, Resources, Project administration. **Malluri Goñas:** Writing – review & editing, Visualization, Supervision, Project administration, Funding acquisition. **Darwin Gómez-Fernández:** Writing – review & editing, Validation, Formal analysis, Data curation.

Declaration of competing interest

The authors declare that they have no known competing financial interests or personal relationships that could have appeared to influence the work reported in this paper.

Appendix

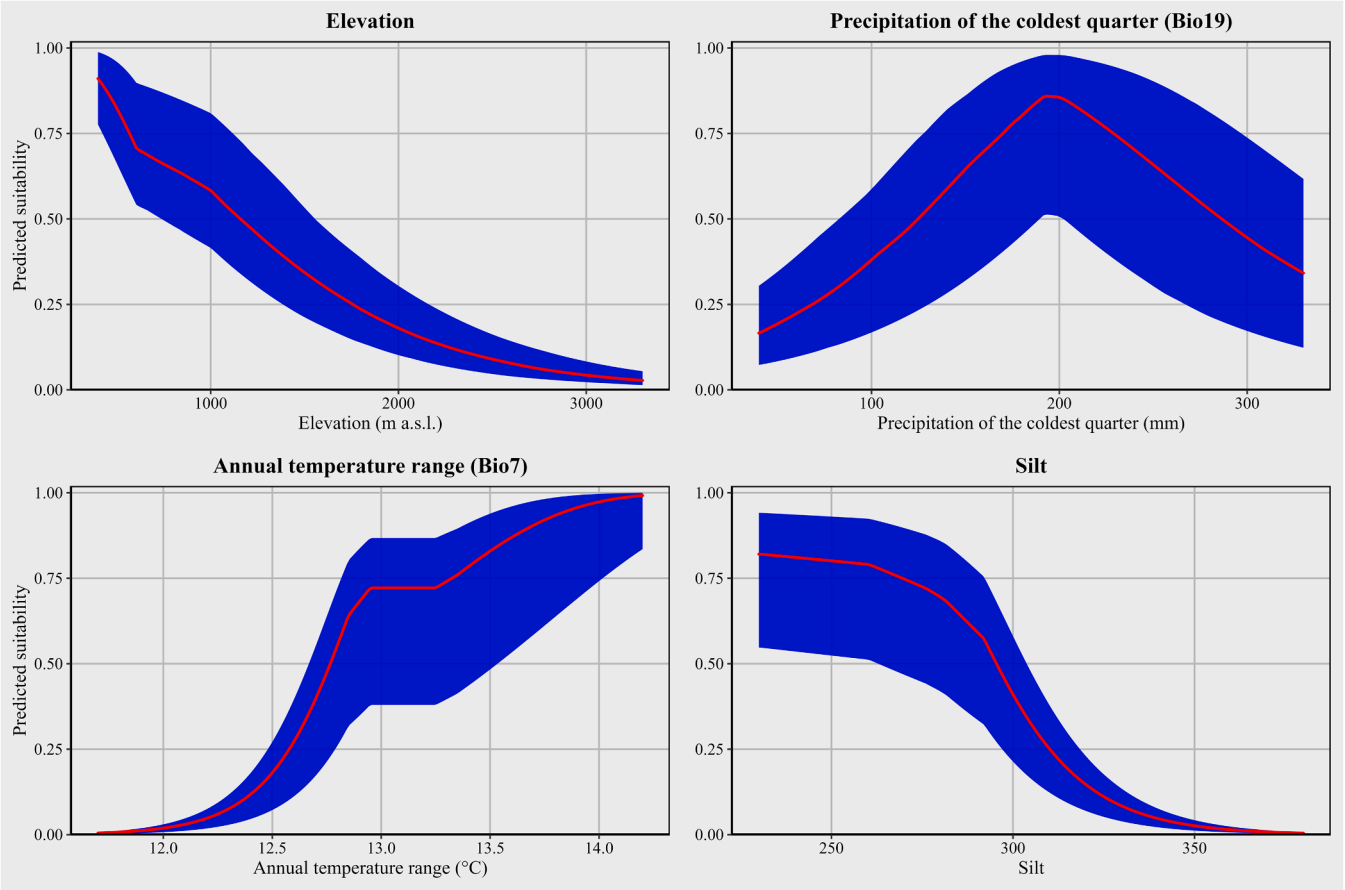

Fig. A.1. Response curves of the most important environmental variables for plantain (*Musa* (AAB), cv. 'Bellaco') derived from the MaxEnt model.

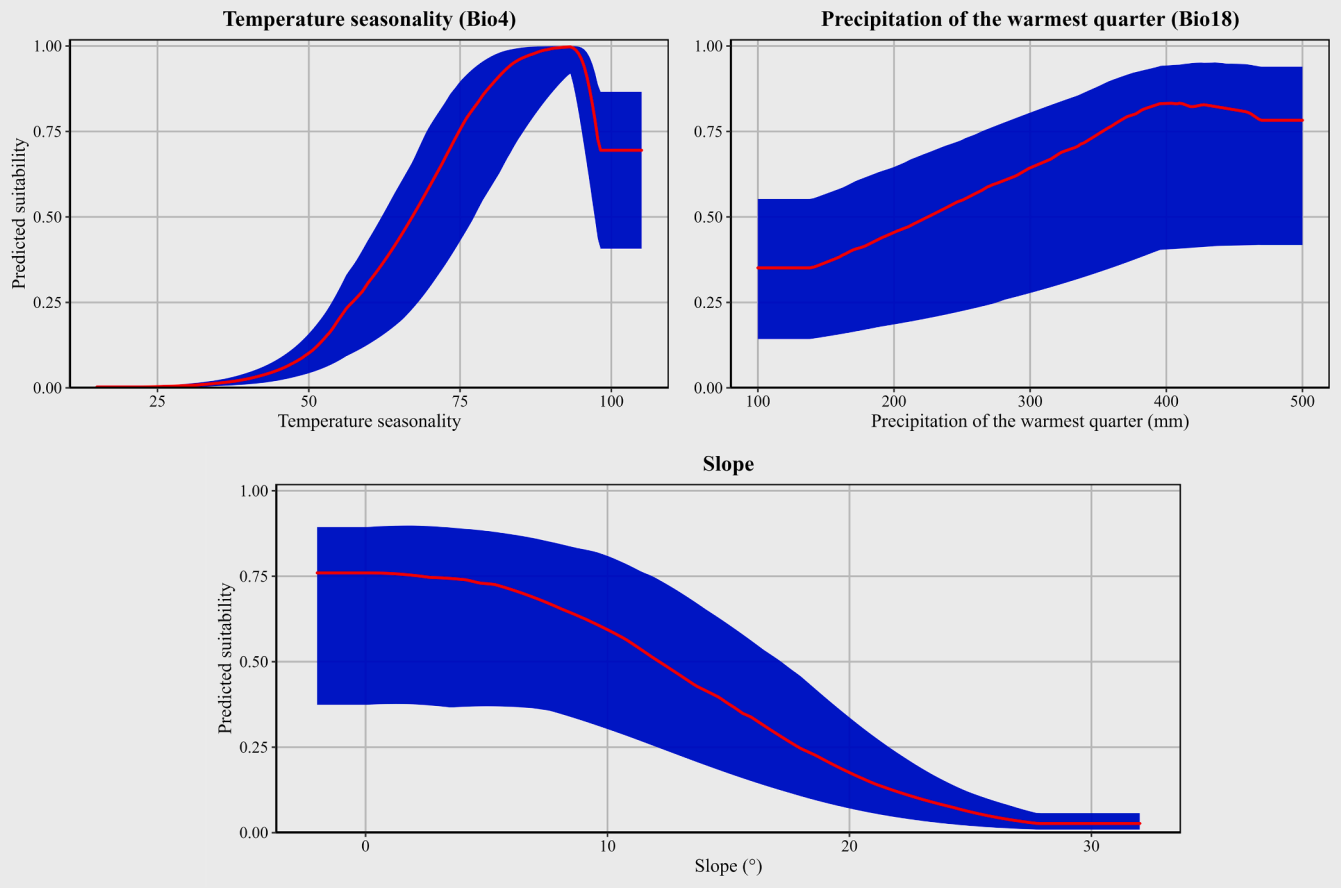

Fig. A.2. Response curves of the most important environmental variables for papaya (*Carica papaya*) derived from the MaxEnt model.

Data availability

The data and code used to support the conclusions of this study can be downloaded at the following link: https://next.data.4tu.nl/private_datasets/M0Ntp6gFYufx3uc4ES1hkN1Ly-x4MH6tZkjM5TBMebY

References

[1] K. Chaturvedi, P. Singh, R. Mehrotra, Application of 'omics technologies in tropical and subtropical fruit crops, Omics Hortic. Crops (Jan. 2022) 119–145, https://doi.org/10.1016/B978-0-323-89905-5.00027-6.

[2] B. Mankhin, M.E. Ara Begum, M.S. Hoq, M.I. Hossain, Determinants of the factors affecting the governance structure choice of the pineapple value chain: a case study on market-based agroforestry in Bangladesh, Heliyon 10 (20) (2024) e39209, https://doi.org/10.1016/J.HELIYON.2024.E39209.

[3] K. Valencia Sandoval, D. Duana Ávila, T.J. Hernández Gracia, Estudio del mercado de papaya mexicana: un análisis de su competitividad (2001-2015), Suma Neg. 8 (18) (2017) 131–139, https://doi.org/10.1016/J.SUMNEG.2017.10.002.

[4] S. Yahalom, C. Guan, Productivity differences in operating breakbulk reefer vessels: the case of a change in vessel hatch design in the banana trade, Case Stud. Transp. Policy 21 (2025) 101517, https://doi.org/10.1016/J.CSTP.2025.101517.

[5] Ministerio de Desarrollo Agrario y Riego (MIDAGRI), "Perfil productivo y competitivo de los principales cultivos del sector." Accessed: Jun. 11, 2025. [Online]. Available: https://goo.su/tdLelX.

[6] A. Chemura, B.T. Mudereri, A.W. Yalew, C. Gornott, Climate change and specialty coffee potential in Ethiopia, Sci. Rep. 11 (1) (Apr. 2021) 1–13, https://doi.org/10.1038/s41598-021-87647-4.

[7] Organización de las Naciones Unidas para la Alimentación y la Agricultura [FAO], El Impacto De Los Desastres En La Agricultura y La Seguridad Alimentaria De La Región América Latina y Caribe, FAO, Roma, Italia, 2016. Accessed: Mar. 01, 2026. [Online]. Available: https://openknowledge.fao.org/handle/20.500.14283/bl463s.

[8] C. Müller, et al., Global gridded crop model evaluation: benchmarking, skills, deficiencies and implications, Geosci. Model. Dev. 10 (4) (Apr. 2017) 1403–1422, https://doi.org/10.5194/gmd-10-1403-2017.

[9] K. Frieler, et al., Understanding the weather signal in national crop-yield variability, Earths Future 5 (6) (2017) 605–616, https://doi.org/10.1002/2016EF000525.

[10] C. Lesk, P. Rowhani, N. Ramankutty, Influence of extreme weather disasters on global crop production, Nature 529 (7584) (2016) 84–87, https://doi.org/10.1038/nature16467.

[11] P. D'Odorico, J.A. Carr, F. Laio, L. Ridolfi, S. Vandoni, Feeding humanity through global food trade, Earths Future 2 (9) (2014) 458–469, https://doi.org/10.1002/2014ef000250.

[12] M. Maetz, M. Aguirre, S. Kim, Y. Matinroshan, G. Pangrazio, V. Pernechele, Food and Agricultural policy trends after the 2008 Food Security crisis: renewed attention to agricultural development, *Rome, Italy*. Accessed: Mar. 01, 2026. [Online]. Available: https://openknowledge.fao.org/handle/20.500.14283/au716e, 2011.

[13] B. Schauberger, et al., Consistent negative response of US crops to high temperatures in observations and crop models, Nat. Commun. 8 (1) (Jan. 2017) 13931, https://doi.org/10.1038/ncomms13931.

[14] E. Vogel, et al., The effects of climate extremes on global agricultural yields, Environ. Res. Lett. 14 (5) (2019) 054010, https://doi.org/10.1088/1748-9326/ab154b.

[15] S. Heinicke, K. Frieler, J. Jägermeyr, M. Mengel, Global gridded crop models underestimate yield responses to droughts and heatwaves, Environ. Res. Lett. 17 (4) (2022) 044026, https://doi.org/10.1088/1748-9326/ac592e.

[16] B.A. Magesa, G. Mohan, H. Matsuda, I. Melts, M. Kefi, K. Fukushi, Understanding the farmers' choices and adoption of adaptation strategies, and plans to climate change impact in Africa: a systematic review, Clim. Serv. 30 (2023) 100362, https://doi.org/10.1016/J.CLISER.2023.100362.

[17] Intergovernmental Panel on Climate Change (IPCC), Climate Change 2022 – Impacts, Adaptation and Vulnerability: Working Group II Contribution to the Sixth Assessment Report of the Intergovernmental Panel On Climate Change, Cambridge University Press, 2023, https://doi.org/10.1017/9781009325844.

[18] W.S. Lavado Casimiro, D. Labat, R. Josyane, J.C. Espinoza, J.L. Guyot, Trends in rainfall and temperature in the Peruvian Amazon-Andes basin over the last 40years (1965-2007), Hydrol. Process. 27 (20) (2013) 2944–2957, https://doi.org/10.1002/hyp.9418.
[19] Gobierno Regional de Cajamarca, Estudio especializado de evaluación del riesgo de desastres y vulnerabilidad al cambio climático, Cajamarca (Dec. 2020). Accessed: Feb. 22, 2026. [Online]. Available: https://www.regioncajamarca.gob.pe/media/portal/IEDID/documento/19405/EE_Evaluaci%C3%B3n_del_Riesgo_de_Desastres_y_Vulnerabilidad_al_C_TLuz7m0.pdf?r=1637873505.
[20] A. Heikkinen, Climate change in the Peruvian Andes: a case study on small-scale farmers' vulnerability in the quillcay river basin, Iberoam. Nord. J. Lat. Am. Caribb. Stud. 46 (1) (2017) 77–88, https://doi.org/10.16993/iberoamericana.211.
[21] Food and Agriculture Organization of the United Nations (FAO), "Tierra y agua." Accessed: Jun. 05, 2025. [Online]. Available: https://www.fao.org/land-water/databases-and-software/crop-information/banana/en/.
[22] V. Cherlinka, "Cultivo de plátano: siembra, mantenimiento y cosecha." Accessed: Jun. 05, 2025. [Online]. Available: https://eos.com/es/blog/cultivo-de-platano/.
[23] P. Jeyakumar, M. Kavino, N. Kumar, K. Soorianathasundaram, Physiological performance of papaya cultivars under abiotic stress conditions, Acta Hortic. 740 (2007) 209–215, https://doi.org/10.17660/ACTAHORTIC.2007.740.25.
[24] Y. Bautista-Bautista, G. Fuentes, S. García-Laynes, F.A. Barredo-Pool, S. Peraza-Echeverria, J.M. Santamaría, CpHSFA2 isolated from a wild native Carica papaya genotype, with potential to confer tolerance to the combined effect of drought stress and heat shock, Plant Physiol. Biochem. 224 (2025) 109925, https://doi.org/10.1016/J.PLAPHY.2025.109925.
[25] F. Tan, L. Zhang, Y. Zhao, F. Bai, J. Zhang, A. Gyilbag, Climatic suitability and development potential of facility agriculture at county-level in China, Sci. Total. Environ. 955 (2024) 177108, https://doi.org/10.1016/J.SCITOTENV.2024.177108.
[26] H. Ray, N. Das, S. Pal, S.C. Pal, S. Mandal, Predicting the potential habitat suitability of mangrove bioindicator species- telescopium telescopium (Linnaeus, 1758) through MaxEnt modelling, Reg. Stud. Mar. Sci. 83 (2025) 104073, https://doi.org/10.1016/J.RSMA.2025.104073.
[27] E. Serra, M. Debolini, H. Fraga, A. Trabucco, V. Mereu, D. Spano, Machine learning and species distribution models for crops: a review, Ecol. Inf. 93 (6) (2026) 103563, https://doi.org/10.1016/j.ecoinf.2025.103563.
[28] X. Li, Z. Wang, S. Wang, Z. Qian, MaxEnt and Marxan modeling to predict the potential habitat and priority planting areas of Coffea arabica in Yunnan, China under climate change scenario, Front. Plant Sci. 15 (Nov. 2024) 1471653, https://doi.org/10.3389/fpls.2024.1471653.
[29] S. Yi, Y. Huang, Z. Liu, Z. Zhu, H. Su, Predicting the potential geographical distribution of mango, an important tropical economic tree species, under current and climate change based on Maxent model, Front. Plant Sci. 16 (Aug. 2025) 1633654, https://doi.org/10.3389/fpls.2025.1633654.
[30] P. Läderach, A. Martinez-Valle, G. Schroth, N. Castro, Predicting the future climatic suitability for cocoa farming of the world's leading producer countries, Ghana and Côte d'Ivoire, Clim. Change 119 (3) (2013) 841–854, https://doi.org/10.1007/s10584-013-0774-8.
[31] N.B. Rojas-Briceño, et al., Land suitability for cocoa cultivation in Peru: AHP and MaxEnt modeling in a GIS environment, Agronomy 12 (12) (Nov. 2022) 2930, https://doi.org/10.3390/AGRONOMY12122930.
[32] J.L. Appelt, T. Saphangthong, P.H. Verburg, J. van Vliet, Climate change impacts on the suitability of lowland and upland crop systems in Lao PDR, Agric. Syst. 226 (2025) 104316, https://doi.org/10.1016/J.AGSY.2025.104316.
[33] G.P. Cárdenas, et al., Current and future distribution of Shihuahuaco (Dipteryx spp.) under climate change scenarios in the Central-Eastern Amazon of Peru, Sustainability 15 (10) (May 2023) 7789, https://doi.org/10.3390/SU15107789.
[34] K. Zhang, Y. Zhang, J. Tao, Predicting the potential distribution of paeonia veitchii (Paeoniaceae) in China by incorporating climate change into a maxent model, Forests 10 (2) (Feb. 2019) 190, https://doi.org/10.3390/F10020190.
[35] M.A. Poma-Sarango, D. Poma-Sarango, L. Guaman, C.G. Chuncho, O. Juela, C. Benavidez-Silva, Distribución potencial de ecosistemas de la Zona Sur del Ecuador: modelización desde un enfoque correlativo, Rev. Estud. Andal. (48) (2024) 8–32, https://doi.org/10.12795/REA.2024.I48.01.
[36] R. Kindt, Ensemble species distribution modelling with transformed suitability values, Environ. Model. Softw. 100 (2018) 136–145, https://doi.org/10.1016/J.ENVSOFT.2017.11.009.
[37] F. Castro-Llanos, G. Hyman, J. Rubiano, J. Ramirez-Villegas, H. Achicanoy, Climate change favors rice production at higher elevations in Colombia, Mitig. Adapt. Strateg. Glob. Chang. 24 (8) (Dec. 2019) 1401–1430, https://doi.org/10.1007/S11027-019-09852-X/FIGURES/10.
[38] R.de S. Nóia Júnior, S. Asseng, C. Müller, J.C. Deswarte, J.P. Cohan, P. Martre, Negative impacts of climate change on crop yields are underestimated, Trends Plant Sci. 30 (11) (2025) 1262–1273, https://doi.org/10.1016/j.tplants.2025.05.002.
[39] A. Hultgren, et al., Impacts of climate change on global agriculture accounting for adaptation, Nature 642 (8068) (2025) 644–652, https://doi.org/10.1038/s41586-025-09085-w.
[40] D. Gómez-Fernández, et al., Territorial zoning as a strategy for sustainable natural resource management in Cajamarca, Northwestern Peru, Ecol. Inf. 92 (2025) 103440, https://doi.org/10.1016/J.ECOINF.2025.103440.
[41] Servicio Nacional de Meteorología e Hidrología del Perú (SENAMHI), Climas del Perú-Mapa de Clasificación Climática Nacional (2021) vol. 1. Lima: Red activa soluciones gráficas S.A.CAccessed: Jun. 11, 2025. [Online]. Available: https://www.senamhi.gob.pe/load/file/01404SENA-4.pdf.
[42] Japan aerospace exploration agency (JAXA), "ALOS PALSAR – corrección radiométrica del terreno".
[43] Servicio Nacional de Meteorología e Hidrología del Perú (SENAMHI), Caracterización y Zonificación Por Aptitud Agroclimática Del Cultivo De Café (coffea arabica) En Las Provincias De Jaén y San Ignacio, Cajamarca, Lima, 2020. Accessed: Jan. 24, 2025. [Online]. Available: https://goo.su/wHfM30.
[44] Gobierno Regional de Cajamarca (GOREC), "Zonificación ecológica económica y ordenamiento territorial en cajamarca." Accessed: Nov. 12, 2025. [Online]. Available: https://zeeot.regioncajamarca.gob.pe/presentacion-zee.
[45] Ministerio de Desarrollo Agrario y Riego (MIDAGRI), "Superficie agrícola del Perú." Accessed: Nov. 12, 2025. [Online]. Available: https://siea.midagri.gob.pe/portal/informativos/superficie-agricola-peruana.
[46] Instituto Nacional de Estadística e Informática (INEI), Cajamarca - Resultados definitivos, Lima, Oct. 2018. Accessed: Jun. 11, 2025. [Online]. Available: https://www.inei.gob.pe/media/MenuRecursivo/publicaciones_digitales/Est/Lib1558/.
[47] Plataforma del Estado Peruano, "Municipalidad provincial de san ignacio - división política." Accessed: Nov. 12, 2025. [Online]. Available: https://www.gob.pe/21069-municipalidad-provincial-de-san-ignacio-division-politica.
[48] V. Proença, et al., Global biodiversity monitoring: from data sources to essential biodiversity variables, Biol. Conserv. 213 (1) (2017) 256–263, https://doi.org/10.1016/j.biocon.2016.07.014.
[49] K.B. Aubry, C.M. Raley, K.S. McKelvey, The importance of data quality for generating reliable distribution models for rare, elusive, and cryptic species, PLoS. One 12 (6) (Jun. 2017) e0179152, https://doi.org/10.1371/journal.pone.0179152.
[50] M. Barbet-Massin, F. Jiguet, C.H. Albert, W. Thuiller, Selecting pseudo-absences for species distribution models: how, where and how many? Methods Ecol. Evol. 3 (2) (2012) 327–338, https://doi.org/10.1111/j.2041-210X.2011.00172.x.
[51] C. Ronquillo, J. Stropp, J. Hortal, OCCUR Shiny application: a user-friendly guide for curating species occurrence records, Methods Ecol. Evol. 15 (5) (2024) 816–823, https://doi.org/10.1111/2041-210X.14271.
[52] R.A. Boria, L.E. Olson, S.M. Goodman, R.P. Anderson, Spatial filtering to reduce sampling bias can improve the performance of ecological niche models, Ecol. Model. 275 (1) (2014) 73–77, https://doi.org/10.1016/j.ecolmodel.2013.12.012.
[53] S.D. Veloz, Spatially autocorrelated sampling falsely inflates measures of accuracy for presence-only niche models, J. Biogeogr. 36 (12) (2009) 2290–2299, https://doi.org/10.1111/j.1365-2699.2009.02174.x.
[54] Y. Fourcade, J.O. Engler, D. Rödder, J. Secondi, Mapping species distributions with MAXENT using a geographically biased sample of presence data: a performance assessment of methods for correcting sampling bias, PLoS. One 9 (5) (May 2014) e97122, https://doi.org/10.1371/journal.pone.0097122.
[55] M.E. Aiello-Lammens, R.A. Boria, A. Radosavljevic, B. Vilela, R.P. Anderson, spThin: an R package for spatial thinning of species occurrence records for use in ecological niche models, Ecography 38 (5) (2015) 541–545, https://doi.org/10.1111/ecog.01132.
[56] N.B. Rojas Briceño, et al., Current and future distribution of five timber forest species in Amazonas, Northeast Peru: contributions towards a restoration strategy, Diversity 12 (8) (Aug. 2020) 305, https://doi.org/10.3390/D12080305.
[57] G.C. Stevens, The latitudinal gradient in geographical range: how so many species coexist in the Tropics, Am. Nat. 133 (2) (1989) 240–256. Accessed: Jun. 17, 2025. [Online]. Available: https://www.jstor.org/stable/2462300.
[58] B. Kharel, et al., Current and future habitat suitability modelling of Bambusa teres outside forest areas in Nepal under climate change scenarios, Adv. Bamboo Sci. 9 (2024) 100112, https://doi.org/10.1016/J.BAMBOO.2024.100112.
[59] F. Beauregard, S. De Blois, Beyond a climate-centric view of plant distribution: edaphic variables add value to distribution models, PLoS. One 9 (3) (Mar. 2014) e92642, https://doi.org/10.1371/journal.pone.0092642.
[60] F. Rota, D. Scherrer, A. Bergamini, B. Price, L. Walthert, A. Baltensweiler, Unravelling the impact of soil data quality on species distribution models of temperate forest woody plants, Sci. Total. Environ. 944 (6) (2024) 173719, https://doi.org/10.1016/j.scitotenv.2024.173719.
[61] T. Lassueur, S. Joost, C.F. Randin, Very high resolution digital elevation models: do they improve models of plant species distribution? Ecol. Model. 198 (1–2) (2006) 139–153, https://doi.org/10.1016/j.ecolmodel.2006.04.004.
[62] D.D. Monache, et al., Mapping local climates in highly heterogeneous mountain regions: interpolation of meteorological station data vs. downscaling of macroclimate grids, Ecol. Inf. 82 (2024) 102674, https://doi.org/10.1016/j.ecoinf.2024.102674.
[63] A. Dubuis, S. Giovanettina, L. Pellissier, J. Pottier, P. Vittoz, A. Guisan, Improving the prediction of plant species distribution and community composition by adding edaphic to topo-climatic variables, J. Veg. Sci. 24 (4) (2013) 593–606, https://doi.org/10.1111/jvs.12002.
[64] S.E. Fick, R.J. Hijmans, WorldClim 2: new 1-km spatial resolution climate surfaces for global land areas, Int. J. Climatol. 37 (12) (2017) 4302–4315, https://doi.org/10.1002/JOC.5086.
[65] R Core Team, R: A Language and Environment for Statistical Computing, R Foundation for Statistical Computing, Vienna, Australia, 2025, 4.4.3. Accessed: Nov. 12, 2025. [Online]. Available: https://www.r-project.org/.
[66] L. Poggio, et al., SoilGrids 2.0: producing soil information for the globe with quantified spatial uncertainty, Soil 7 (1) (Jun. 2021) 217–240, https://doi.org/10.5194/SOIL-7-217-2021.
[67] M.E. Turek, et al., Global mapping of volumetric water retention at 100, 330 and 15 000 cm suction using the WoSIS database, Int. Soil Water Conserv. Res. 11 (2) (2023) 225–239, https://doi.org/10.1016/J.ISWCR.2022.08.001.

[68] T.G. Farr, et al., The shuttle radar topography mission, Rev. Geophys. 45 (2) (Jun. 2007) 2004, https://doi.org/10.1029/2005RG000183.
[69] S. Chen, C. You, Z. Zhang, Z. Xu, Predicting the potential distribution of Quercus oxyphylla in China under climate change scenarios, Forests 15 (6) (Jun. 2024) 1033, https://doi.org/10.3390/F15061033/S1.
[70] C.F. Dormann, et al., Collinearity: a review of methods to deal with it and a simulation study evaluating their performance, Ecography 36 (1) (Jan. 2013) 27–46, https://doi.org/10.1111/J.1600-0587.2012.07348.
[71] B.B. Hanberry, Practical guide for retaining correlated climate variables and unthinned samples in species distribution modeling, using random forests, Ecol. Inf. 79 (5) (2024) 102406, https://doi.org/10.1016/j.ecoinf.2023.102406.
[72] B. Naimi, N.A.S. Hamm, T.A. Groen, A.K. Skidmore, A.G. Toxopeus, Where is positional uncertainty a problem for species distribution modelling? Ecography 37 (2) (2014) 191–203, https://doi.org/10.1111/J.1600-0587.2013.00205.X.
[73] R. Valavi, J. Elith, J.J. Lahoz-Monfort, G. Guillera-Arroita, blockCV: an r package for generating spatially or environmentally separated folds for k-fold cross-validation of species distribution models, Methods Ecol. Evol. 10 (2) (2019) 225–232, https://doi.org/10.1111/2041-210X.13107.
[74] V. Chugani, "Guía completa para la validación cruzada K-Fold," datacamp. Accessed: Jun. 24, 2025. [Online]. Available: https://www.datacamp.com/es/tutorial/k-fold-cross-validation.
[75] J.A. Hanley, B.J. McNeil, The meaning and use of the area under a receiver operating characteristic (ROC) curve, Radiology 143 (1) (1982) 29–36, https://doi.org/10.1148/RADIOLOGY.143.1.7063747.
[76] O. Allouche, A. Tsoar, R. Kadmon, Assessing the accuracy of species distribution models: prevalence, kappa and the true skill statistic (TSS), J. Appl. Ecol. 43 (6) (Dec. 2006) 1223–1232, https://doi.org/10.1111/J.1365-2664.2006.01214.
[77] X. Gao, et al., Prediction of the potential distribution of a raspberry (Rubus idaeus) in China based on MaxEnt model, Sci. Rep. 14 (1) (Dec. 2024) 1–11, https://doi.org/10.1038/S41598-024-75559-Y.
[78] M. Luo, et al., Predicting potentially suitable bletilla striata habitats in China under future climate change scenarios using the optimized MaxEnt model, Sci. Rep. 15 (1) (Dec. 2025) 1–13, https://doi.org/10.1038/S41598-025-08372-W.
[79] K.B. Hebbar, A.S. P, S. Jose V, R. S V, R. Bhat, Predicting current and future climate suitability for arecanut (Areca catechu L.) in India using ensemble model, Heliyon 10 (4) (2024) e26382, https://doi.org/10.1016/J.HELIYON.2024.E26382.
[80] H. Tatebe, et al., Description and basic evaluation of simulated mean state, internal variability, and climate sensitivity in MIROC6, Geosci. Model. Dev. 12 (7) (Jul. 2019) 2727–2765, https://doi.org/10.5194/gmd-12-2727-2019.
[81] S. Yukimoto, et al., MRI MRI-ESM2.0 model output prepared for CMIP6 CMIP, Earth Syst. Grid Fed. (2019), https://doi.org/10.22033/ESGF/CMIP6.621.
[82] IPCC, Summary for policymakers, Clim. Change Phys. Sci. Basis (Jul. 2021) 3–32, https://doi.org/10.1017/9781009157896.001.
[83] Z. Li, T. Liu, Y. Huang, J. Peng, Y. Ling, Evaluation of the CMIP6 precipitation simulations over global land, Earths. Future 10 (8) (2022) e2021EF002500, https://doi.org/10.1029/2021EF002500.
[84] T. Emmenegger, et al., Evaluating tropical precipitation relations in CMIP6 models with ARM data, J. Clim. 35 (19) (Sep. 2022) 6343–6360, https://doi.org/10.1175/JCLI-D-21-0386.1.
[85] V. Eyring, et al., Overview of the Coupled Model Intercomparison Project phase 6 (CMIP6) experimental design and organization, Geosci. Model. Dev. 9 (5) (May 2016) 1937–1958, https://doi.org/10.5194/gmd-9-1937-2016.
[86] B.C. O'Neill, et al., The Scenario Model Intercomparison Project (ScenarioMIP) for CMIP6, Geosci. Model. Dev. 9 (9) (Sep. 2016) 3461–3482, https://doi.org/10.5194/GMD-9-3461-2016.
[87] D.A. Randall et al., "Climate models and their evaluation," United Kingdom and New York, 2007.
[88] C. Tebaldi, R. Knutti, The use of the multi-model ensemble in probabilistic climate projections, Philos. Trans. R Soc. Math. Phys. Eng. Sci. 365 (1857) (2007) 2053–2075, https://doi.org/10.1098/rsta.2007.2076.
[89] C. O'Rourke, et al., Diagnostic accuracy of SUVmax in predicting malignancy of supraclavicular lymph nodes from primary oesophageal cancer, Eur. J. Radiol. 125 (2020) 108860, https://doi.org/10.1016/J.EJRAD.2020.108860.
[90] A. Kallner, Formulas, Lab. Stat. (Jan. 2018) 1–140, https://doi.org/10.1016/B978-0-12-814348-3.00001-0.
[91] R. Zhao, S. Wang, S. Chen, Predicting the potential habitat suitability of Saussurea species in China under future climate scenarios using the optimized Maximum Entropy (MaxEnt) model, J. Clean. Prod. 474 (2024) 143552, https://doi.org/10.1016/J.JCLEPRO.2024.143552.
[92] R. Sun, G. Tong, Q. Zhang, L. Xu, Z. Sang, Y. Li, A study on the suitable areas for growing apricot kernels in China based on the MaxEnt model, Sustainability 15 (12) (Jun. 2023) 9635, https://doi.org/10.3390/su15129635.
[93] D. Ochola, et al., Mapping spatial distribution and geographic shifts of East African highland banana (Musa spp.) in Uganda, PLoS. One 17 (2) (Feb. 2022) e0263439, https://doi.org/10.1371/JOURNAL.PONE.0263439.
[94] B.G. Tikuye, R.L. Ray, Predicting future corn suitability zones under climate change scenarios in the United States of America, J. Agric. Food Res. 22 (2025) 102129, https://doi.org/10.1016/J.JAFR.2025.102129.
[95] N. Khan, R.L. Ray, G.R. Sargani, M. Ihtisham, M. Khayyam, S. Ismail, Current progress and future prospects of agriculture technology: gateway to sustainable agriculture, Sustainability 13 (9) (Apr. 2021) 4883, https://doi.org/10.3390/SU13094883.
[96] R. Manners, et al., Suitability of root, tuber, and banana crops in Central Africa can be favoured under future climates, Agric. Syst. 193 (2021) 103246, https://doi.org/10.1016/J.AGSY.2021.103246.
[97] S.J. Tulowiecki, N. LaDuke, Models reveal shifting distribution of climatic suitability for pawpaw (Asimina triloba [L.] Dunal) cultivation under future climate change scenarios, Sci. Hortic. 338 (2024) 113837, https://doi.org/10.1016/J.SCIENTA.2024.113837.
[98] E. Espinosa Trujillo, A.J. Gámez Vázquez, M.A. Avila Perches, F. Palemón Alberto, J. Hernández-Ruíz, Distribución geográfica potencial de papaya silvestre cultivada en México, Rev. Mex. Cienc. Agric. 9 (7) (Nov. 2018) 1377–1388, https://doi.org/10.29312/remexca.v9i7.550.
[99] F. Xin, J. Liu, C. Chang, Y. Wang, L. Jia, Evaluating the influence of climate change on sophora moorcroftiana (Benth.) baker habitat distribution on the tibetan plateau using maximum entropy model, Forests 12 (9) (Sep. 2021) 1230, https://doi.org/10.3390/F12091230/S1.
[100] G.E. Manzanilla-Quijada, E.J. Treviño-Garza, O.A. Aguirre-Calderón, J.I. Yerena-Yamallel, U. Manzanilla-Quiñones, Distribución potencial actual y futura e identificación de áreas aptas para la conservación de Cedrela odorata L. en la península de Yucatán, Rev. Chapingo. Ser. Cienc. For. Ambiente. 26 (3) (Aug. 2020) 391–408, https://doi.org/10.5154/R.RCHSCFA.2019.10.075.
[101] D.W. Turner, J.A. Fortescue, D.S. Thomas, Environmental physiology of the bananas (Musa spp.), Braz. J. Plant Physiol. 19 (4) (2007) 463–484, https://doi.org/10.1590/S1677-04202007000400013.
[102] E.F. Coelho, et al., Water regimes on soil covered with plastic film mulch and relationships with soil water availability, yield, and water use efficiency of papaya trees, Agric. Water. Manag. 269 (2022) 107709, https://doi.org/10.1016/J.AGWAT.2022.107709.
[103] M. Vantyghem, R. Merckx, B. Stevens, R. Hood-Nowotny, R. Swennen, G. Dercon, The potential of stable carbon isotope ratios and leaf temperature as proxies for drought stress in banana under field conditions, Agric. Water. Manag. 260 (2022) 107247, https://doi.org/10.1016/J.AGWAT.2021.107247.
[104] G. Blomme, A. Tenkouano, R. Swennen, The effect of soil bulk density on root and overall plant development in six banana varieties [Online]. Available: https://www.researchgate.net/publication/285737488, 2002.
[105] G. Blomme, R. Swennen, G. Soka, L. Turyagyenda, A. Tenkouano, Relationship between root and shoot growth traits during the plant crop and first ratoon in banana and plantain (Musa spp.) and its implications for perennial cultivation on degraded Ultisols in south-eastern Nigeria [Online]. Available: www.biosciences.elewa.org, Jan. 2008.
[106] S.K. Sweet, N.L. Bassuk, B.M. Miller, Deep compost amendment reduces soil bulk density resulting in improved growth of urban Gymnocladus dioicus trees over time, Urban. For. Urban. Green 108 (2025) 128822, https://doi.org/10.1016/J.UFUG.2025.128822.
[107] P. Bhardwaj, K. Jarial, R.S. Jarial, D. Kumar, Effect of weather parameters on the development of post harvest rots of Papaya, Int. J. Curr. Microbiol. App. Sci. 9 (10) (2020) 855–867, https://doi.org/10.20546/ijcmas.2020.910.102.
[108] G.A.R. de Souza, et al., Supra-optimal temperatures induce photochemical leaf damage and reduce photosynthetic O2 evolution in Carica papaya L, Environ. Exp. Bot. 203 (2022) 105051, https://doi.org/10.1016/J.ENVEXPBOT.2022.105051.
[109] P.L. Saran, R. Choudhary, I.S. Solanki, S. Ercisli, Der einfluss der temperatur auf die samen-keimung bei Papaya unter den subtropischen Bedingungen Indiens, Erwerbs. Obstbau. 58 (3) (2016) 199–202, https://doi.org/10.1007/s10341-016-0275-9.
[110] G. Rana, P. Deb, B. Dowarah, R.L. Sahu, Effect of temperature on seed germination of Papaya (Carica papaya L.) under the laboratory condition, Environ. Ecol. 42 (3B) (2024) 1301–1305, https://doi.org/10.60151/ENVEC/HJVA6364.
[111] V.Q. Silvestre, et al., Impacto de los cambios climáticos y uso de suelo, en la distribución de las especies de géneros endémicos de Asteraceae de Arequipa, Arnaldoa 26 (1) (2019) 71–96, https://doi.org/10.22497/ARNALDOA.261.26105.
[112] P. Arribas, et al., Species vulnerability under climate change, a new challenge for biodiversity conservation, Ecosistemas 21 (3) (Sep. 2012) 79–84, https://doi.org/10.7818/ECOS.2012.21-3.10.
[113] L. Nkurunziza, C.A. Watson, I. Öborn, H.G. Smith, G. Bergkvist, J. Bengtsson, Socio-ecological factors determine crop performance in agricultural systems, Sci. Rep. 10 (1) (Dec. 2020) 1–12, https://doi.org/10.1038/S41598-020-60927-1;SUBJMETA.
[114] R.A. Labarta, D. White, E. Leguía, W. Guzmán, J. Soto, La agricultura en la Amazonia ribereña del río Ucayali: ¿una zona productiva pero poco rentable? Acta Amaz. 37 (2) (2007) 177–186, https://doi.org/10.1590/S0044-59672007000200002.
[115] V. Varma, D.P. Bebber, Climate change impacts on banana yields around the world, Nat. Clim. Chang. 9 (10) (2019) 752–757, https://doi.org/10.1038/S41558-019-0559-9.
[116] U. Rippke, et al., Timescales of transformational climate change adaptation in sub-Saharan African agriculture, Nat. Clim. Chang. 6 (6) (2016) 605–609, https://doi.org/10.1038/NCLIMATE2947.

[117] S.C. Davies, et al., Addressing uncertainty when projecting marine species' distributions under climate change, Ecography 2023 (11) (2023) e06731, https://doi.org/10.1111/ECOG.06731.
[118] H. Mugiyo, et al., Mapping the spatial distribution of underutilised crop species under climate change using the MaxEnt model: a case of KwaZulu-Natal, South Africa, Clim. Serv. 28 (2022) 100330, https://doi.org/10.1016/J.CLISER.2022.100330.
[119] T. Akafu, D. Korecha, W. Garedew, A. Amare, Modeling the current land suitability and future dynamics for coffee (Coffea Arabica L.) cultivation under climate change scenarios in western Ethiopia with MaxEnt model, Earth. Syst. Environ. (Jun. 2025) 1–18, https://doi.org/10.1007/S41748-025-00689-W/TABLES/3.
[120] J.C. Stanton, R.G. Pearson, N. Horning, P. Ersts, H.R. Akçakaya, Combining static and dynamic variables in species distribution models under climate change, Methods Ecol. Evol. 3 (2) (2012) 349–357, https://doi.org/10.1111/j.2041-210X.2011.00157.x.
[121] J.A. Rivera, G. Arnould, Evaluation of the ability of CMIP6 models to simulate precipitation over Southwestern South America: climatic features and long-term trends (1901–2014), Atmos. Res. 241 (2020) 104953, https://doi.org/10.1016/j.atmosres.2020.104953.
[122] J. Patiño, et al., Spatial resolution impacts projected plant responses to climate change on topographically complex islands, Divers. Distrib. 29 (10) (Oct. 2023) 1245–1262, https://doi.org/10.1111/ddi.13757.